MAURÍCIO CUNHA ALMEIDA LEITE

# ACTIVATED BIOCHAR AND HUMIC ACID AS ADDITIVES IN SOLUBLE PHOSPHATE FERTILIZER

Dissertação apresentada à Universidade Federal de Viçosa, como parte das exigências do Programa de Pós-Graduação em Solos e Nutrição de Plantas, para obtenção do título de *Magister Scientiae.*

VIÇOSA
MINAS GERAIS – BRASIL
2019

**Ficha catalográfica preparada pela Biblioteca Central da Universidade Federal de Viçosa - Câmpus Viçosa**

T
L533a
2019

Leite, Maurício Cunha Almeida, 1992-
Activated biochar and humic acid as additives in soluble phosphate fertilizer / Maurício Cunha Almeida Leite. – Viçosa, MG, 2019.
vii, 50 f. : il. (algumas color.) ; 29 cm.

Texto em inglês.
Orientador: Edson Marcio Mattiello.
Dissertação (mestrado) - Universidade Federal de Viçosa.
Inclui bibliografia.

1. Fertilizantes fosfatados. 2. Biocarvão. 3. Ácido húmico. 4. Adsorção. 5. Dessorção. I. Universidade Federal de Viçosa. Solos e nutrição de plantas. Programa de Pós-Graduação em Solos e Nutrição de Plantas. II. Título.

CDD 22. ed. 631.85

MAURÍCIO CUNHA ALMEIDA LEITE

# ACTIVATED BIOCHAR AND HUMIC ACID AS ADDITIVES IN SOLUBLE PHOSPHATE FERTILIZER

Dissertação apresentada à Universidade Federal de Viçosa, como parte das exigências do Programa de Pós-Graduação em Solos e Nutrição de Plantas, para obtenção do título de *Magister Scientiae*.

APROVADA: 3 de julho de 2019.

Leônidas Carrijo Azevedo Melo

Teresa Cristina Fonseca da Silva

LeonardusVergütz
(Coorientador)

Edson Marcio Mattiello
(Orientador)

DEDICATÓRIA

*Aos meus pais Euclides (in memoriam) e Rosana e meu irmão Alexandre,*
***Dedico.***

# AGRADECIMENTOS

Aos meus pais, Rosana e Euclides, por todo amor, apoio, incentivo e cuidados constantes.

A toda minha família, por me apoiarem em todas as minhas decisões e por transmitir grande amor por mim, mesmo em distância.

À Universidade Federal de Viçosa e ao Departamento de Solos (DPS), pela oportunidade de realização do Mestrado; e ao CNPq (Conselho Nacional de Desenvolvimento Científico e Tecnológico) pela bolsa concedida e apoio a pesquisa nacional.

Ao professor Edson Marcio Mattiello, pela confiança depositada, experiências e ensinamentos transmitidos e por todo apoio nos momentos que mais precisei.

Aos demais professores do DPS pela participação na minha formação e pelo exemplo de profissionalismo; e aos técnicos e funcionários do departamento pela ajuda e bom convívio.

A minha equipe e amigos de laboratório, Fabiane, Patrícia, Isabela, Karol, Denison e Vinicius, que nunca hesitaram em me ajudar e me fazer mais feliz.

A todos os colegas e amigos que tive o prazer de conhecer em Viçosa, pessoas incríveis com histórias incríveis.

Em especial, a família que escolhi como minha em Viçosa, Maria, David e Daniel, que sempre me apoiaram nos bons e nos maus momentos. Permitiram-me crescer como pessoa e como amigo, vocês têm minha eterna gratidão e amizade.

SUMÁRIO

ABSTRACT

LEITE, Maurício Cunha Almeida, M.Sc., Universidade Federal de Viçosa, July, 2019. **Activated biochar and humic acid as additives in soluble phosphate fertilizer.** Adviser: Edson Marcio Mattiello. Co-advisers: Leonardus Vergütz and Wedisson Oliveira Santos.

Phosphate fertilization has low agronomic efficiency in clay tropical soils rich in Fe and Al oxyhydroxides, due to the their high phosphate sorption capacity. Therefore, the use of coating substances in fertilizers capable of preventing phosphorus (P) sorption in soil can be strategic to increase the efficiency of these products. The present work was aimed at evaluating the use of humic acid and a chemically modified biochar as additives in granules of monoammonium phosphate (MAP), as well as to study P diffusivity, P release in soil and its effect on plants growth. Biochar from eucalyptus sawdust was produced and chemically modified with zinc chloride, aluminum chloride and iron chloride, in order to select the biochar with the highest potential of P sorption. Zinc biochar (ZnBC) showed the highest sorptive potential and it was selected for further evaluated for sorption and desorption analysis. After evaluating the kinetic potential of sorption e desorption of P, the ZnBC was compared with humic acid (HA) as additives in granules of phosphate fertilizer (MAPZnBC and MAPHA respectively) by mean of diffusivity trial, P release in soil and an agronomic experiment. It was observed that the treatments MAPHA and MAPZnBC did not effectively change the diffusivity, but were able to increase the contents of P-soil release in comparison with the control treatment (MAP) in the granulesphere soil. However, in the agronomic evaluation, the additives had no effect on the dry matter of the crops, and only MAPHA was able to increase the P uptake by the plants.

# RESUMO

LEITE, Maurício Cunha Almeida, M.Sc., Universidade Federal de Viçosa, julho de 2019. **Biocarvão ativado e ácido húmico como aditivos em fertilizante fosfatado solúvel.** Orientador: Edson Marcio Mattiello. Coorientadores: Leonardus Vergütz and Wedisson Oliveira Santos.

A adubação fosfatada apresenta baixa eficiência agronômica em solos tropicais mais argilosos, ricos em oxihidróxidos de Fe e Al, devido à alta capacidade de adsorção química de ortofosfato desses adsorventes. Portanto, o uso de revestimentos em fertilizantes capazes de prevenir a adsorção química de P no solo pode ser estratégico para aumentar a eficiência desses produtos. Neste sentido, o presente trabalho tem como objetivo avaliar o uso de ácido húmico e biocarvão ativado quimicamente como aditivos em grânulos de fertilizante fosfato monoamônico solúvel (MAP), assim como, estudar a difusividade e teores de P na região do grânulo e o efeito desses tratamentos no crescimento de plantas. No intuito de selecionar o biocarvão com maior potencial de adsorção de P, três tipos de biocarvões foram produzidos com diferentes agentes de ativação química, como cloreto de zinco, cloreto de alumínio e cloreto de ferro. Após a produção e analises qualitativas, apenas o biocarvão ativado quimicamente com zinco (BCZn) mostrou alto potencial adsortivo e por isso foi selecionado para analises mais especificas sobre a sua capacidade de adsorção e dessorção. Após avaliar o potencial cinético de adsorção e dessorção de P, o BCZn foi comparado com um ácido húmico (AH) em grânulos de fertilizante (MAP) como aditivos (MAPBCZn e MAPAH) por meio de ensaios de difusividade, liberação de P no solo e eficiência agronômica. Por meio dessas avaliações concluiu-se que os tratamentos MAPAH e MAPBCZn não alteraram de forma efetiva a difusividade dos grânulos, toda via, foram capazes de aumentar o teor de P disponível na região do grânulo. Porém, no experimento de avaliação agronômica não foram observados efeitos positivos quando os tratamentos foram comparados com o controle MAP para o parâmetro matéria seca, sendo que apenas o tratamento MAPAH foi capaz de aumentar o conteúdo de P nas plantas.

# GENERAL INTRODUCTION

Since the last decades in Brazil, a significant increase in use of phosphorus fertilizers have been observed (Lu and Tian, 2017), having a substantial contribution to the green revolution in the country. Nevertheless, the amount of phosphorus (P) applied as fertilizer in soil is much higher than the crop demand (Withers et al., 2018) due to the high P-adsorbing capacity of tropical soils, especially clay soils rich in Fe and Al oxihydroxides (Novais and Smyth, 1999).

The reduction of the interaction of P ions with the oxidic matrix of soil appears to be a possibility to increase the efficiency of P fertilization in highly weathered soils. On this perspective, the beneficial effect of adding soil organic materials reducing P adsorption is well known (Fink et al., 2016). Another promising strategy is the use of technologies as coating linked to fertilizers, which P-protecting and increase its availability to plants (Benício et al., 2017).

Biochar (BC) and humic acid (HA) are example of organic materials that can be used as fertilizers coating to reduce the contact between P and soil. Biochar is a product obtained from the thermal degradation of organic wastes under minimal oxygen conditions (Lehmann, 2014). Despite the large number of uses that biochar offers itself, it is possible to improve its characteristics of interest through activations. During the production of activated biochar, the chemical activation may be carried out before or after the pyrolysis process. When the chemical activation is performed prior to pyrolysis, the activating agent acts on the formation of the biochar structure, and chemical activation occurs simultaneously with the pyrolysis (Zhang et al., 2007; Veksha et al., 2014; Altintig and Kirkil, 2016).

In order to improve the adsorption capacity of anions, such as phosphate, various chemical activations have been studied (Zhang et al., 2012; Morales et al., 2013; Wang et al., 2015; Liu et al., 2016). It is interesting to note that activated materials have a high degree of microporosity, which differs greatly in the surface area and in the charge generated on its surface (Altintig and Kirkil, 2016). On the other hand, HA can compete for adsorption sites of P by conditioner sorption that occurs in soil through the action of molecules able to compete with P through connection sites, covering clay minerals, reducing the area of these adsorbents or creating new adsorption sites (Borggaard et al., 1990; Gerke, 2010; Kleber et al., 2015; Fink et al., 2016).

The kinetics process depends on the adsorbate-adsorbent interaction and system condition (Yuh-Shan, 2004). Using the stirred-flow analysis technique, it is possible to evaluate the capacity of the BC and HA in the P sorption, without interference of loss of potential or solution buffering, as in batch experiments, due to the constant renewal of the adsorbate and agitation of the solution during the analysis (Bar-Tal et al., 1990).

Thus, one of the aim of this work was synthesize and characterize an activated biochar with three different agents ($ZnCl_2$, $AlCl_3$ and $FeCl_3$). Furthermore, the biochar with the highest P sorption capacity was used to evaluate the P kinetics using an stirred-flow apparatus. In the context, we hypothesized that the use of organic additives as coatings of soluble P fertilizer has strong potential to interact with the surface of the granule, as well as the granulesphere and decreasing the sorption of P by Fe and Al oxyhydroxides. Thus, we aimed to evaluate the performance of soluble P fertilizer coated with organic additives, such as activated BC and HA. Specifically, we assessed the P-diffusivity in soil, P-availability in the region surrounding the granule and the efficiency of recovery of P by plants in successive cultivation.

## REFERENCES


Altintig E, Kirkil S. Preparation and properties of Ag-coated activated carbon nanocomposites produced from wild chestnut shell by ZnCl2 activation. J Taiwan Inst Chem Eng. Elsevier B.V.; 2016;63:180–188.

Bar-Tal A, Feigenbaum S, Sparks DL, Pesek JD. Analyses of Adsorption Kinetics Using a Stirred-Flow Chamber: I. Theory and Critical Tests. Soil Sci Soc Am J. 1990;54:1273.

Benício LPF, Constantino VRL, Pinto FG, Vergütz L, Tronto J, Da Costa LM. Layered Double Hydroxides: New Technology in Phosphate Fertilizers Based on Nanostructured Materials. ACS Sustain Chem Eng. 2017;5:399–409.

Borggaard O.K, Jdrgensen SS, Moberg JP, Raben-lange B. Influence of organic matter on phosphate adsorption by aluminium and iron oxides in sandy soils. J Soil Sci. 1990;41:443–449.

Fink, Jessé R, Inda AV, Tiecher T, Barrón V. Iron oxides and organic matter on soil phosphorus availability. Cienc e Agrotecnologia. 2016;40:369–379.

Fink JR, Inda AV, Tiecher T, Barrón V. Iron oxides and organic matter on soil phosphorus availability. Ciência e Agrotecnologia. 2016;40:369–379.

Gai X, Wang H, Liu J, Zhai L, Liu S, Ren T, Liu H. Effects of feedstock and pyrolysis temperature on biochar adsorption of ammonium and nitrate. PLoS One. Public Library of Science; 2014;9:e113888.

Gerke J. Humic (organic matter)-Al(Fe)-phosphate complexes: An underestimated phosphate form in soils and source of plant-available phosphate. Soil Sci. 2010;175:417–425.

Kleber M, Eusterhues K, Keiluweit M, Mikutta C, Mikutta R, Nico PS. Mineral-Organic Associations: Formation, Properties, and Relevance in Soil Environments [Internet]. Adv. Agron. Elsevier Ltd; 2015.

Lehmann J. Biochar for Environmental Management. Biochar Environ. Manag. Routledge; 2014.

Liu SB, Tan XF, Liu YG, Gu YL, Zeng GM, Hu XJ, Wang H, Zhou L, Jiang LH, Zhao B Bin. Production of biochars from Ca impregnated ramie biomass (Boehmeria nivea (L.) Gaud.) and their phosphate removal potential. RSC Adv. Royal Society of Chemistry; 2016;6:5871–5880.

Lu C, Tian H. Global nitrogen and phosphorus fertilizer use for agriculture production in the past half century: shifted hot spots and nutrient imbalance. Earth Syst Sci Data. 2017;9:181–192.

Morales MM, Comerford N, Guerrini IA, Falcão NPS, Reeves JB. Sorption and desorption of phosphate on biochar and biochar-soil mixtures. Soil Use Manag. John Wiley & Sons, Ltd (10.1111); 2013;29:306–314.

Veksha A, Zaman W, Layzell DB, Hill JM. Enhancing biochar yield by co-pyrolysis of bio-oil with biomass: Impacts of potassium hydroxide addition and air pretreatment prior to co-pyrolysis. Bioresour Technol. Elsevier Ltd; 2014;171:88–94.

Wang Z, Guo H, Shen F, Yang G, Zhang Y, Zeng Y, Wang L, Xiao H, Deng S. Biochar produced from oak sawdust by Lanthanum (La)-involved pyrolysis for adsorption of ammonium (NH 4+ ), nitrate (NO 3- ), and phosphate (PO 43- ). Chemosphere. Elsevier Ltd; 2015;119:646–653.

Withers PJA, Rodrigues M, Soltangheisi A, De Carvalho TS, Guilherme LRG, Benites VDM, Gatiboni LC, De Sousa DMG, Nunes RDS, Rosolem CA, Andreote FD, Oliveira A De, Coutinho ELM, Pavinato PS. Transitions to sustainable management of phosphorus in Brazilian agriculture. Sci Rep. Springer US; 2018;8:1–13.

Yuh-Shan H. Citation review of Lagergren kinetic rate equation on adsorption reactions. Scientometrics. 2004;59:171–177.

Zhang L, Xu S, Zhao W, Liu S. Co-pyrolysis of biomass and coal in a free fall reactor. Fuel. 2007;86:353–359.

Zhang M, Gao B, Yao Y, Xue Y, Inyang M. Synthesis of porous MgO-biochar nanocomposites for removal of phosphate and nitrate from aqueous solutions. Chem Eng J. Elsevier B.V.; 2012;210:26–32.

Zheng H, Wang Z, Deng X, Herbert S, Xing B. Impacts of adding biochar on nitrogen retention and bioavailability in agricultural soil. Geoderma. Elsevier; 2013;206:32–39.

# Selection of different chemical activation agents of biochar to obtain high adsorption capacity of phosphorus

# Selection of different chemical activation agents of biochar to obtain high adsorption capacity of phosphorus

Maurício Cunha Almeida Leite[a], Fabiane Carvalho Ballotin[a], Edson Marcio Mattiello[a], LeonardusVergütz[a], Wedisson Oliveira Santos[a], Denison Pogorzelski[a]

[a] Department of Soil Science, Universidade Federal de Viçosa, Viçosa, Brazil.

ABSTRACT

Eucalyptus sawdust was used as a precursor for preparing activated biochar by using different chemical activation agents: zinc chloride, aluminum chloride and iron chloride. The effects of activation parameters, i.e., total contents, remaining-P, elemental analysis, surface area and pore volume were evaluated for all materials. In order to select the most promising material as phosphorus (P) adsorbent, the results of remaining-P and surface area were used. Zinc biochar (ZnBC) was selected and it was characterized by FTIR, SEM and by kinetics trial in stirred-flow system, to evaluate sorption and desorption. The maximum surface area of ZnBC was 940 $m^2$ $g^{-1}$, achieved by using the impregnation ($ZnCl_2$:biomass) ratio of 1:1, pyrolysis at 500 °C with residence time of 60 min. The ZnBC presented an area three times higher than control biochar (without activation), besides a higher adsorption capacity of P, therefore has potential as P adsorbent.

**Keywords:** Biochar, chemical activation, phosphorus, zinc, adsorption, desorption.

# INTRODUCTION

Plant biomass is a renewable resource that has been the focus of many studies, due to its versatility of chemical use and functionalized materials. Despite the large number of uses that biochar offers itself, it is possible to improve characteristics of interest in these materials through activations. During the production of activated biochar, physical, chemical or both processes are used. The chemical activation may be carried out before or after the pyrolysis process. When the chemical activation is performed prior to pyrolysis, the activating agent acts on the formation of the biochar structure, and chemical activation occurs simultaneously with the pyrolysis (Zhang et al., 2007; Veksha et al., 2014; Altintig e Kirkil, 2016).

The use of biochar without chemical activation to produce an P adsorbent matrix is not very effective (Zheng et al., 2013; Gai et al., 2014). In order to improve the adsorption capacity of anions, such as phosphate, various chemical activations have been studied (Zhang et al., 2012; Morales et al., 2013; Wang et al., 2015; Liu et al., 2016). It is interesting to note that activated materials have a high degree of microporosity, which differs greatly in the surface area and in the charge generated on its surface (Altintig and Kirkil, 2016).

Adsorption kinetics depends on the adsorbate-adsorbent interaction and system condition (Yuh-Shan, 2004). In order to evaluate the biochars as sorption matrix, a study of the kinetics between the adsorbent and the adsorbate is necessary. Using the "stirred flow" analysis technique, it is possible to evaluate the capacity of the biochar in the P sorption, without interference of loss of potential or solution buffering, as in batch experiments, due to the constant renewal of the adsorbate and agitation of the solution during the analysis (Bar-Tal et al., 1990).

Thus, the aim of this paper was the synthesis and characterization of activated biochar with three different agents ($ZnCl_2$, $AlCl_3$ and $FeCl_3$). Furthermore, the biochar with the most promising characteristics to adsorb P was used to evaluate the P kinetics on continuous flow trial and compare their performance against a biochar without chemical activation.

# MATERIALS AND METHODS

*Biochar synthesis*

The selected raw material for the production of biochar was Eucalyptus sawdust (*Eucalyptus spp.*). The sawdust was crushed and passed through a 30 mm sieve and dried in a closed air circulation oven at 105° C to constant weight. After drying, the material was impregnated with the different materials ($ZnCl_2$, $AlCl_3$ and $FeCl_3$) to perform the chemical activation.

*Chemical Impregnation*

The biochar impregnation was performed using zinc chloride ($ZnCl_2$), aluminum chloride ($AlCl_3$) and iron chloride ($FeCl_3$) separately. For each impregnation, a concentration solution of 1.5 mol $L^{-1}$ in deionized water was used for each agent. Thus the biomass (200 g) was layered in 1 L of solution. During the impregnation process, the eucalyptus sawdust was mixed with each solution and stirred at approximately 80 °C for 7 h. The mixtures were dried on a heating plate at 200 °C until most of the liquid was evaporated. The residual moisture was removed in air closed circulation oven at 60 °C.

*Pyrolysis and activation process*

The eucalyptus sawdust after chemical impregnation was subjected to slow pyrolysis with a heating rate of 10 ° C $min^{-1}$ until it reaches the temperature of 500° C, and maintained at that temperature for 1 h. The pyrolysis process was done in a muffle on anoxic environment. After the production, the biochar was passed through constant washing in deionized water until the pH value and electrical conductivity remained constant. The final product was milled and passed in 80 mesh (177µm) and stored for analysis.

*Characterization*

The characterizations remaining-P and surface area were used to select the most promising biochar as the adsorbent matrix of P. From these results, only ZnBC was selected, and other evaluations were made.

The total content of biochar (BC), zinc biochar (ZnBC), aluminum biochar (AlBC) and iron biochar (FeBC) were performed by a the digestion method as described elsewhere (Enders and Lehmann, 2012) . The total contents were determined by inductively coupled plasma optical emission spectrometry (ICP-OES) (supplementary material-Table S1). The elemental analysis of C, H and N was done in a Perkin-Elmer 2400 Series II CHNS/O Analyzer. The pH of the biochar in water suspension was determined at a 1:20 (w/v) ratio (Zhao et al., 2013). Electrical conductivity (EC) and pH of the suspension in water was performed considering the ratio 1:20 (m / v), after intermittent shaking (90 rpm) for 24 h (Zhao et al., 2013).

The specific surface area (SSA) was estimated by adsorption of $N_2$ at 77 K (Quantachrome, model NOVA 2200e) by the BET model (Brunauer et al., 1938) (P / P0 between 0.05-0.25). The samples were prepared as described by ASTM (2012). The pore size and distribution were estimated by the BJH model (Barrett et al., 1951) in the range 0.99-0.50 relative pressure in the desorption isotherm. Data was processed by NOVAWin software.

A qualitative investigation of functional groups was performed by attenuated total reflectance Fourier transform infrared spectroscopy (ATR- FTIR) (Jasco spectrometer, model FT/IR-4100), spectra were collected at wavenumber range of 4000 to 500 cm $^{-1}$ with a resolution of 4 cm$^{-1}$ and 256 scans. The morphology of the material was analyzed by scanning electron microscopy (SEM), Jeol, model JSM 6010-LA, with the images generated by the LEO 1430 VP. To complete evaluate of the composition, the technique of Energy-dispersive X-ray spectroscopy (EDS) was carried out with the detector type Silicon Drift Detector. The characterization the crystalline phases of the biochars were accomplished by X-ray diffraction (XRD) analyses performed in a Shimadzu XRD-6000 diffractometer, using a graphite crystal monochromator to select Cu-Kα1 radiation with $\lambda$ = 1.5406 Å and a step way from 0.02°/s, with 2$\theta$ angle between 4° and 70°.

Remaining P analysis (P-rem) was adapted from Alvarez et al., 2000, using a solution containing 0.01 mol L$^{-1}$ $CaCl_2$ and 60 mg L$^{-1}$ $KH_2PO_4$, 0.5 g of the biochar was immersed in 75 mL of the P-Ca solution, stirred for 5 min at 120 rpm and left resting for

16 hours. The P contained in the fractions was measured by molecular absorption spectrometry (Braga, J. M, Defelipo, 1974).

*Sorption and desorption kinetics*

The kinetic study of P was carried out in a continuous flow system as described by Fernández-Calviño et al., (2010). The system consists of reservoirs of solutions, piston pump (HPLC - Thermo Scientific, ultimate 3000), acrylic reactor (internal volume of 17 mL) mounted on a magnetic stirrer (400 rpm) and an automatic fraction collector (Gilson, FC 203B fraction collector) (Benício et al., 2017). A mass of 0.75 g of biochar was added to the reactor for each evaluation and a background solution (10 µmol $L^{-1}$ KCl in ultra-pure water) was used to complete the reactor volume, being used a filter of de 0,22 µm pore diameter to retain biochar in the reactor. After that, the kinetics experiment was started using a solution containing 500 µmol $L^{-1}$ of P and 10 µm $L^{-1}$ KCl (as background) in ultrapure water. After 180 min the solution flow was stopped and started the of 10 µmol $L^{-1}$ KCl in ultrapure water for the desorption. Both solutions were adjusted to pH 6 and the solution flow was kept constant (1 mL $min^{-1}$). We also used blank controls (without biochar) in which the sorption-desorption experiments were the same. The evaluation was promoted during 170 min, both for adsorption and desorption

The P contained in the solution leaving the reactor was measured by molecular absorption spectrometry (Braga, J. M. Defelipo, 1974). The kinetic curves were obtained through average data, from three replicates per type of biochar (BC and ZnBC). The sorption (Equation 1) and desorption (Equation 2) were calculated according to Fernández-Calviño et al., (2010):

$$q(i) = \left\{\sum_{j=1}^{i}\left[\frac{(P1(j)-P2(j))\Delta tj}{Ve}\right] + [P1\,(i+1) - P2(i+1)]\right\}\frac{Ve}{m} \qquad \text{Eq. 1}$$

$$q(i) = \left\{\sum_{j=1}^{i}\left[\frac{(P2(j)-P1(j))\Delta tj}{Ve}\right] + [P2\,(i+1) - P1(i+1)]\right\}\frac{Ve}{m} \qquad \text{Eq. 2}$$

where q(i) = adsorption or desorption (mg $g^{-1}$) accumulated in iΔt time (min) (Δt = collection time of each alíquota from the reactor); P1 (i) and P2 (i) = phosphorus concentration in each aliquot in the absence and presence of BC or ZnBC (mg $L^{-1}$),

respectively; J = flow rate (L $min^{-1}$); Ve = the effective volume of the solution reactor (L); and m = mass of BC or ZnBC (g).

From the sorption-desorption curves, it was possible to analyze the kinetic of adsorption/ desorption of the P by the BC and ZnBC. In order to distinguish kinetics equation based on concentration of solution and adsorption capacity of a pseudo-first-order model (Largergren, 1898) was used and can be represented by the equation 3 and 4:

$$\frac{dq_{ads}}{dt} = k_{ads}\,(q_{max} - q_{ads}) \qquad \text{Eq. 3}$$

$$\frac{dq_{des}}{dt} = k_{des}\,(q_{max} - q_{des}) \qquad \text{Eq. 4}$$

in which $q_{ads}$ (mg $g^{-1}$) is the P adsorbed at time $t$, $q_{des}$ (mg $g^{-1}$) is the P desorbed at time $t$, $q_{max}$ is the maximum concentration of P adsorbed or desorbed at equilibrium (mg $g^{-1}$), $k_{ads}$ ($min^{-1}$) and $k_{des}$ ($min^{-1}$) are the adsorption and desorption rate constant respectively.

Integration of Equations 3 and 4 with the conditions $t = 0$ to $t = t$, $q_{ads} = 0$ to $q_{ads} = q_{ads}$ and $q_{ades} = 0$ to $q_{des} = q_{des}$:

$$q_{ads}=q_{max}(1 - e^{-kt}) \qquad \text{Eq. 5}$$

$$q_{des} = q_{max}\,(1 - e^{-kt}) \qquad \text{Eq. 6}$$

## RESULTS AND DISCUSSION

### *Production, characterization and selection of activated biochar*

The yield of biochar production can be influenced by characteristics such as feedstock and pyrolysis temperature (Mašek et al., 2013). The different chemical agents did not change the yield (Table 1). Furthermore, the decrease of biochars yields was due to losses of C as $CO_2$ as examples.

The BC presented low contents of micro and macronutrients, while ZnBC, FeBC and AlBC presented higher contents for the impregnated elements (Table 1). ZnBC, AlBC and FeBC showed a decrease of 31%, 57% and 52% on C content, respectively as

compared to pristine BC. The carbon content decreased on the activated material due to release of CO and $CO_2$ (Caturla et al., 1991).

The remaining P (Table 2) showed that the BC did not adsorbed P as expected, different from other materials, in which no P was founded on the solution, showing that the materials have potential as P adsorbents.

The materials surface area (Table 2) showed that BC, FeBC and AlBC presented similar surface areas, different from ZnBC, which presented the largest surface area among the studed materials (940 $m^2$ $g^{-1}$). Furthermore, the materials pore volume increased in activated biochars. The low area of FeBC and AlBC could be related to ions blocking the pores as a consequence for not have been totally removed. Furthermore, longer carbonization times are required to increase porosity (Mohanty et al., 2006).

As pointed out by Wang et al., (2017) the pyrolysis process generated Zn oxides, which may contribute to increase the surface area, once causes the enlargement of the pore structure by the metal oxide particles entering into the pores (Zaini et al., 2009). Moreover, Zn addition could help on the formation of hydroxyl groups on ZnO particles (Noei et al., 2008). Biochar activation with $ZnCl_2$ at 1 hour and 500 °C produced a material with the highest surface area (>800 $m^2g^{-1}$) (Mohanty et al., 2006), as observed in our study. These results are important when choosing a material with high P sorption capacity, since among the factors that govern the sorption, the surface area is very relevant (Cooney, 1998). Thus, due to the low remaning-P and high surface area, the ZnBC was chosen to be characterized in more detail and to perform the P kinetic test compared to BC.

**Table 1.** Chemical and physical properties of biochar (BC), zinc biochar (ZnBC), aluminium biochar (AlBC) and iron biochar (FeBC).

| Physical and chemical properties | BC | ZnBC | AlBC | FeBC |
|---|---|---|---|---|
| C ($g\ kg^{-1}$)[1] | 84.29 | 57.87 | 36.21 | 40.57 |
| H ($g\ kg^{-1}$)[1] | 3.25 | 1.69 | 3.08 | 2.26 |
| N ($g\ kg^{-1}$)[1] | 0.23 | 0.33 | 0.15 | 0.15 |
| Surface area ($m^2\ g^{-1}$)[2] | 305 | 940 | 154 | 222 |
| Pore volume ($cm^3\ g^{-1}$)[3] | 0.02 | 0.06 | 0.07 | 0.06 |
| P remaining ($mg\ L^{-1}$)[4] | 56.42 | 0.01 | 1.16 | 0.03 |
| pH ($H_2O$)[5] | 7.65 | 6.06 | 4.82 | 4.51 |
| Yield ($g\ kg^{-1}$) | 530 | 540 | 520 | 480 |
| P ($g\ kg^{-1}$)[6] | 1.26 | 1.07 | 0.85 | 1.19 |
| Zn ($g\ kg^{-1}$)[6] | 0.94 | 49.59 | 0.00 | 0.19 |
| Al ($g\ kg^{-1}$)[6] | 0.66 | 2.69 | 100.11 | 6.42 |
| Fe ($g\ kg^{-1}$)[6] | 2.35 | 10.99 | 0.94 | 62.34 |

(1) elemental analysis, (2,3) estimated by $N_2$ adsorption.(4) adapted from Alvarez et al., (2000), (5)biochar:water ratio of 1:20, (6) plasma optical emission spectrometry (ICP-OES).

*FTIR and DRX*

The Figure 2 shows the FTIR of the BC and ZnBC. There are common peaks characteristic of coal materials in the spectrum of BC, the band in 1696 $cm^{-1}$ is due to C=O stretching. Furthermore, in 1568 $cm^{-1}$ it was observed C=C stretching due to coal aromatic ring. It was also seen a band related to C-O stretching in 1163 $cm^{-1}$. Besides that, on ZnBC IR spectrum, a wide band in 3400 $cm^{-1}$ related to adsorbed water was founded, corresponds to stretching of the O-H group (Huang et al., 2009), mainly in the carboxylic acid functional group. Probably water could have been adsorbed on ZnO surface. The bands in 1555 $cm^{-1}$ (C=C stretching) and 1167 $cm^{-1}$ (C-O stretching) were also verified. These results are in accordance with reported data (Tang et al., 2015; Wang et al., 2017).

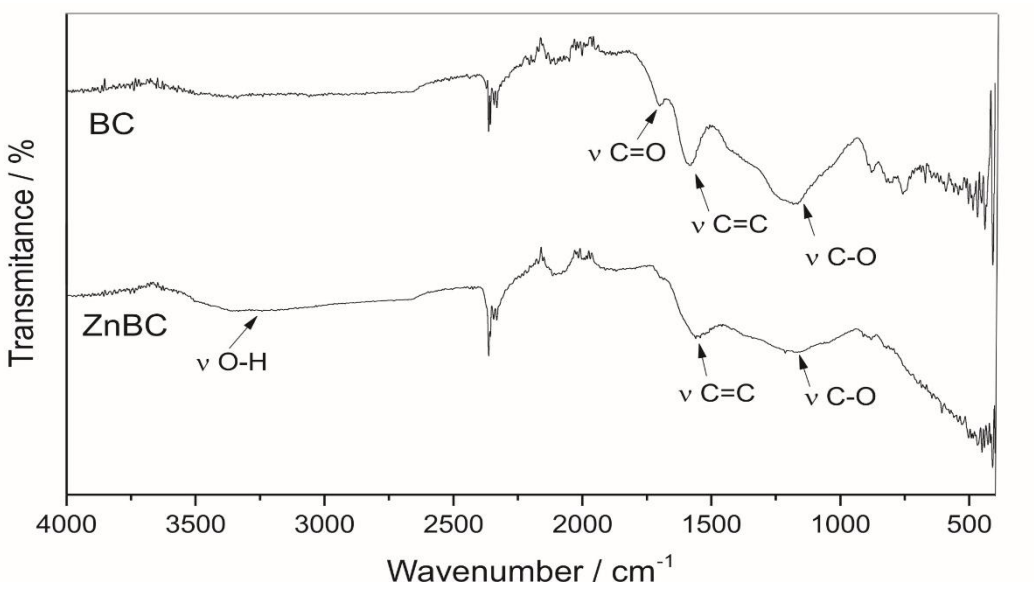


**Fig. 2.** Infrared spectrum of BC (biochar) and ZnBC (activated Zn biochar).

In order to confirm the materials crystallinity an X ray diffraction was performed (Figure 3). The BC clearly shows a broad peak in 10-30 °, due to diffraction of amorphous carbon (Liou, 2009) and two peaks 44.13 and 64,23 °, related to Fe (JCPDS 1-152). It is interesting to note that ZnBC does not present the amorphous peak due to amorphous carbon. Furthermore, for the ZnBC can be seen ZnO (JCPDS 36-1451) and $Zn_5(OH)_8Cl_2H_2O$, simoncolleite phase (JCPDS 7-155), which are due to impregnation and activation process.

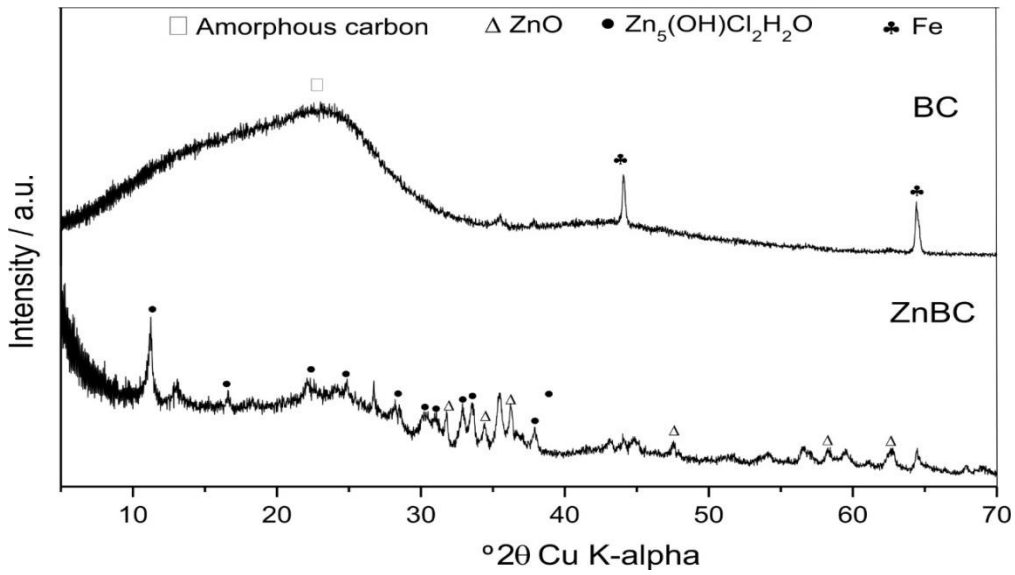


**Figure 3.** X-ray diffratograms of samples BC and ZnBC.

*Scanning electron microscopy (SEM)*

The Scanning electron microscopy (SEM) technique was used to investigate the surface of biochars (Figure 4). Significant differences on BC and ZnBC surfaces were observed. BC presented elongated particles from 10-50 μm. The ZnBC, however, presented an irregular surface with cavities, due to the activation process.

The $ZnCl_2$ acts as a catalyst in the polymerization reactions between compounds formed during pyrolysis and aromatic hydrocarbons in the structure (Ahmadpour and Do, 1997). The compounds formed during this process are large molecules consisting of these reactions, and by the effect of temperature, move away from the structure, and leave a porous structure (Say and Güzel, 2016). Similar results were reported in other studies (Mohanty et al., 2006; Uçar et al., 2009). The EDS analysis was also performed (Figure.5). For the ZnBC, a large quantity of Zn well-dispersed was found, showing that impregnation process was homogeneous.

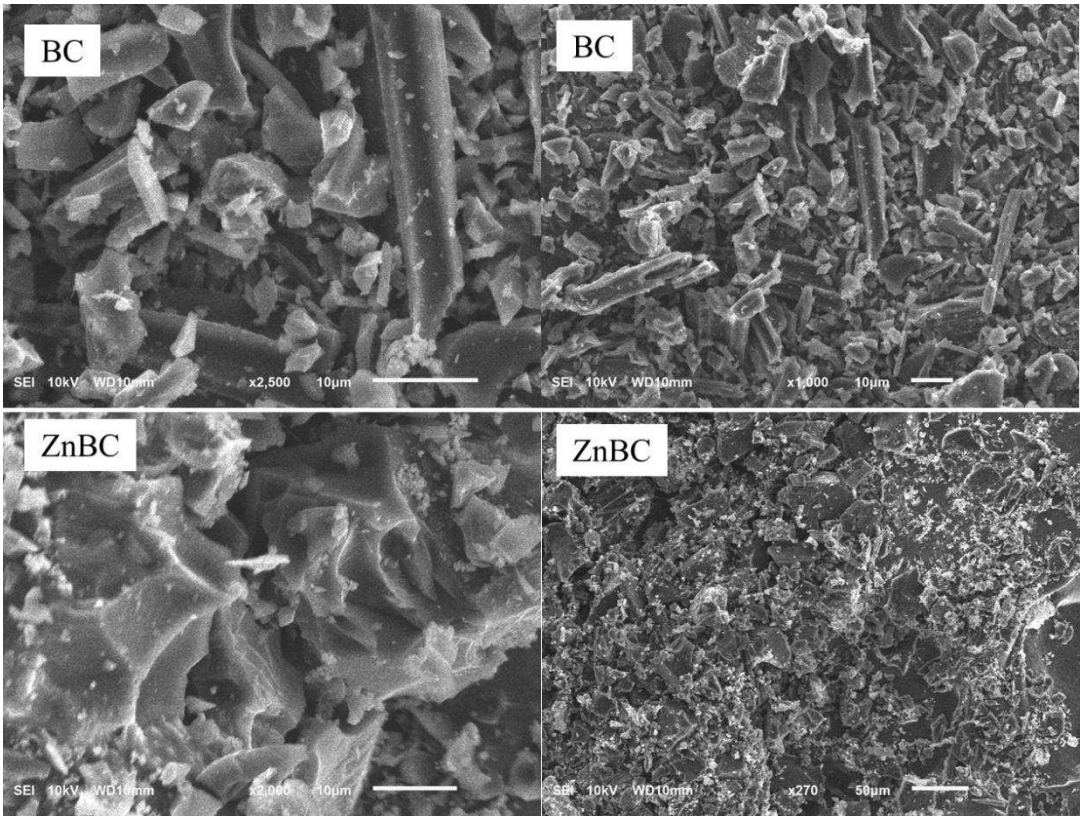


**Figure. 4.** Scanning electron microscopy (SEM) images of *Eucalyptus* biochar (BC) and of actvated zinc biochar (ZnBC).

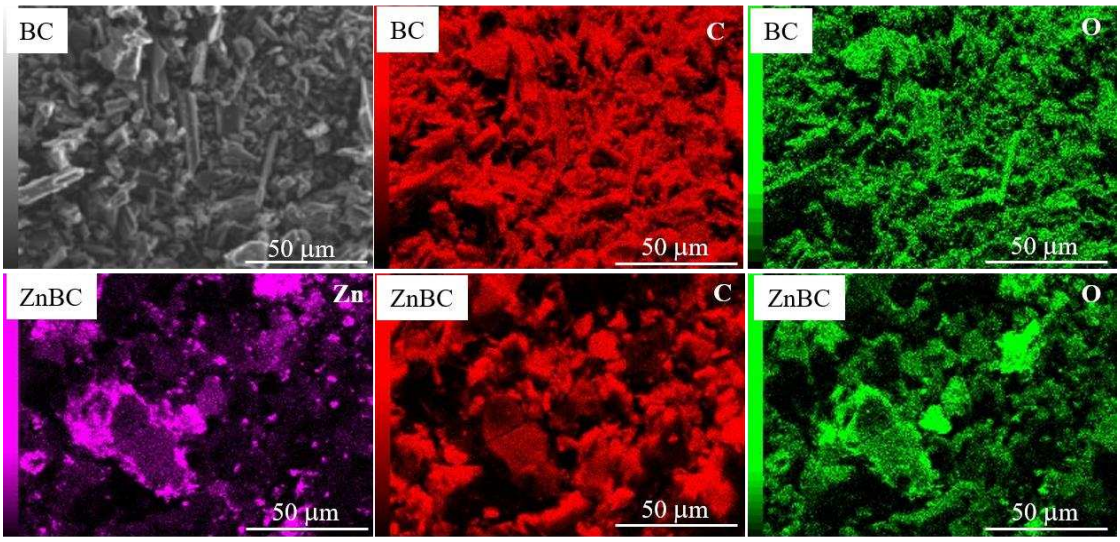


**Figure. 5.** EDS analyses of materials BC and ZnBC, showing C, O and Zn elements.

*Sorption and desorption kinetics*

The ZnBC showed P sorption capacity of approximately 100 mg $g^{-1}$ , which is about 2.5-fold greater than non-activated biochar (≅40 mg $g^{-1}$ P) (Figure 6). The material also showed high P desorption fraction, indicating high reversibility of the sorption in the organomineral complex of the biochar. Evaluating the cumulative data of P sorption and desorption it is possible to notice that the fast sorption tends to grow up to 40 and 80 min to BC and ZnBC, respectively (Figure 6). The maximum sorption capacity observed by the cumulative sorption was not possible to reach by the evaluation time on the stirred-flow, therefore, using the parameters of the Largergren (1898) model, it is possible to estimate the maximum of P adsorbed and desorbed in equilibrium (*q max*). For adsorption, the BC *q max* reached 52 mg $g^{-1}$ and for ZnBC 126 mg $g^{-1}$ of P (Table 3). For desorption, it was observed that the BC obtained *qmax* of 14 mg $g^{-1}$ and ZnBC 48 mg $g^{-1}$ of P (Table 3). Also, observing the accumulated values (Figure 6) for ZnBC it is possible to notice that in the maximum time of evaluation (180 min) only 38 % of P adsorbed had been desorbed.

Comparing the values of the surface area and pore volume (Table 1) with *q max* (table 4), it is possible to observe that as much the ZnBC surface area and pore volume increased by the chemical activation, its *q max* also increased proportionally, presenting values 3 times higher for area and pores, and 2.4 times higher for *q max* than BC.

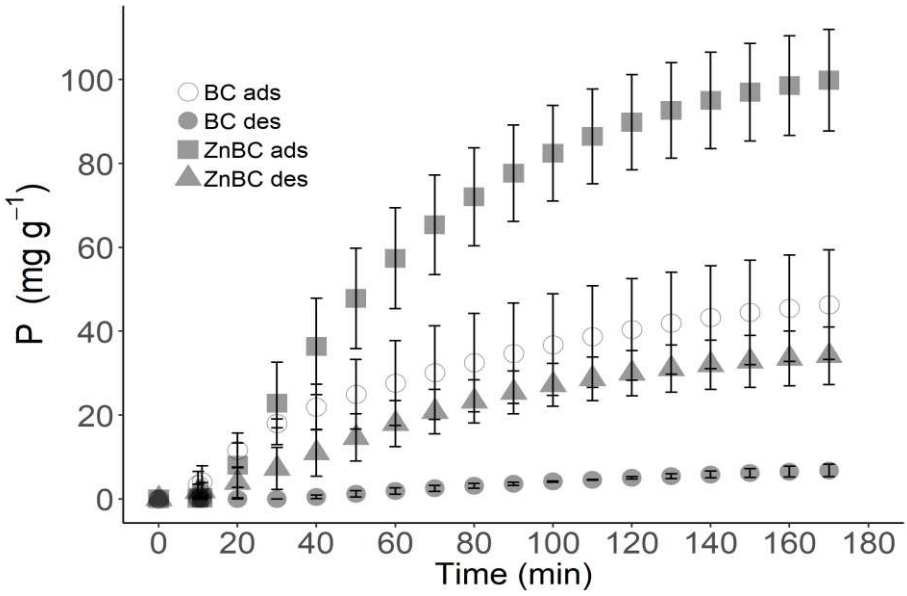


**Figure 6**. Phosphorus (P) cumulative adsorption (ads) and desorption (des) by biochar (BC) or zinc biochar (ZnBC) in stirred-flow system. Data shown as the mean values of duplicates with bars to indicate the standard error of the mean.

**Table 2.** Parameters of P adsorption and desorption by BC and ZnBC by Largergren model.

| Biochars | Adsorption | | | Desorption | | |
|---|---|---|---|---|---|---|
| | $q_{max}$ (mg g$^{-1}$) | $k$ (min$^{-1}$) | $R^2$ | $q_{max}$ (mg g$^{-1}$) | $k$ (min$^{-1}$) | $R^2$ |
| BCZn | 126 | $1.0 \times 10^{-2}$ | 0.98 | 48 | $8.0 \times 10^{-3}$ | 0.98 |
| BC | 52 | $1.3 \times 10^{-2}$ | 0.99 | 14 | $3.0 \times 10^{-3}$ | 0.98 |

*CONCLUSIONS*

The chemical activation of Eucalyptus sawdust showed to be a promising method to increase the surface area and thus, adsorption capacity of the materials when compared to non-activated biochar.

Due to its higher P-adsorption capacity and surface area, the material activated with Zn showed better results than material treated with Al and Fe. It seems that the cavities and irregular surface can be resulted from the $ZnCl_2$ impregnation and carbonization process.

Moreover, the stirred flow trial showed that ZnBC can adsorb 126 mg g$^{-1}$ of P while BC has a capacity of only 52 mg g$^{-1}$. These results showed that ZnBC is a potential material to be used on contaminants removal or even combined with fertilizers in order to increase P availability for plants.

*Acknowledgment*

The authors gratefully acknowledge funding received from Conselho Nacional de Desenvolvimento Científico e Tecnológico (CNPq) and Fertilizantes Heringer.

## REFERENCE

Altintig E, Kirkil S. Preparation and properties of Ag-coated activated carbon nanocomposites produced from wild chestnut shell by ZnCl2 activation. J Taiwan Inst Chem Eng. Elsevier B.V.; 2016;63:180–188.

Bar-Tal A, Feigenbaum S, Sparks DL, Pesek JD. Analyses of Adsorption Kinetics Using a Stirred-Flow Chamber: I. Theory and Critical Tests. Soil Sci Soc Am J. 1990;54:1273.

Barrett EP, Joyner LG, Halenda PP. The determination of pore volume and area distributions in porous substances. I. Computations from nitrogen isotherms. J Am Chem Soc. ACS Publications; 1951;73:373–380.

Benício LPF, Constantino VRL, Pinto FG, Vergütz L, Tronto J, Da Costa LM. Layered Double Hydroxides: New Technology in Phosphate Fertilizers Based on Nanostructured Materials. ACS Sustain Chem Eng. 2017;5:399–409.

Brunauer S, Emmett PH, Teller E. Adsorption of gases in multimolecular layers. J Am Chem Soc. ACS Publications; 1938;60:309–319.

Caturla F, Molina-Sabio M, Rodríguez-Reinoso F. Preparation of activated carbon by chemical activation with ZnCl2. Carbon N Y. Pergamon; 1991;29:999–1007.

Cooney DO. Adsorption design for wastewater treatment. CRC press; 1998.

Enders A, Lehmann J. Comparison of Wet-Digestion and Dry-Ashing Methods for Total Elemental Analysis of Biochar. Commun Soil Sci Plant Anal. 2012;43:1042–1052.

Fernández-Calviño D, Pérez-Novo C, Bermúdez-Couso A, López-Periago E, Arias-Estévez M. Batch and stirred flow reactor experiments on Zn sorption in acid soils. Cu competition. Geoderma. Elsevier B.V.; 2010;159:417–424.

Gai X, Wang H, Liu J, Zhai L, Liu S, Ren T, Liu H. Effects of feedstock and pyrolysis temperature on biochar adsorption of ammonium and nitrate. PLoS One. Public Library of Science; 2014;9:e113888.

Huang G, Shi JX, Langrish TAG. Removal of Cr (VI) from aqueous solution using activated carbon modified with nitric acid. Chem Eng J. Elsevier; 2009;152:434–439.

Liou T-H. Development of mesoporous structure and high adsorption capacity of biomass-based activated carbon by phosphoric acid and zinc chloride activation. Chem Eng J. Elsevier; 2009;158:129–142.

Liu SB, Tan XF, Liu YG, Gu YL, Zeng GM, Hu XJ, Wang H, Zhou L, Jiang LH, Zhao B Bin. Production of biochars from Ca impregnated ramie biomass (Boehmeria nivea (L.) Gaud.) and their phosphate removal potential. RSC Adv. Royal Society of Chemistry; 2016;6:5871–5880.

Mašek O, Brownsort P, Cross A, Sohi S. Influence of production conditions on the yield and environmental stability of biochar. Fuel. 2013;103:151–155.

Mohanty K, Das D, Biswas MN. Preparation and characterization of activated carbons from Sterculia alata nutshell by chemical activation with zinc chloride to remove phenol from wastewater. Adsorption. Kluwer Academic Publishers; 2006;12:119–132.

Morales MM, Comerford N, Guerrini IA, Falcão NPS, Reeves JB. Sorption and desorption of phosphate on biochar and biochar-soil mixtures. Soil Use Manag. John Wiley & Sons, Ltd (10.1111); 2013;29:306–314.

Noei H, Qiu H, Wang Y, Löffler E, Wöll C, Muhler M. The identification of hydroxyl groups on ZnO nanoparticles by infrared spectroscopy. Phys Chem Chem Phys. The Royal Society of Chemistry; 2008;10:7092.

Say H, Güzel F. High surface area mesoporous activated carbon from tomato processing solid waste by zinc chloride activation: process optimization, characterization and dyes adsorption. J Clean Prod. 2016;113:995–1004.

Tang J, Lv H, Gong Y, Huang Y. Preparation and characterization of a novel graphene/biochar composite for aqueous phenanthrene and mercury removal. 2015;

Uçar S, Erdem M, Tay T, Karagöz S. Preparation and characterization of activated carbon produced from pomegranate seeds by ZnCl2 activation. Appl Surf Sci. North-Holland; 2009;255:8890–8896.

Veksha A, Zaman W, Layzell DB, Hill JM. Enhancing biochar yield by co-pyrolysis of bio-oil with biomass: Impacts of potassium hydroxide addition and air pretreatment prior to co-pyrolysis. Bioresour Technol. Elsevier Ltd; 2014;171:88–94.

Wang P, Tang L, Wei X, Zeng G, Zhou Y, Deng Y, Wang J, Xie Z, Fang W. Synthesis and application of iron and zinc doped biochar for removal of p-nitrophenol in wastewater and assessment of the influence of co-existed Pb(II). Appl Surf Sci. 2017;392:391–401.

Wang Z, Guo H, Shen F, Yang G, Zhang Y, Zeng Y, Wang L, Xiao H, Deng S. Biochar produced from oak sawdust by Lanthanum (La)-involved pyrolysis for adsorption of ammonium (NH 4+ ), nitrate (NO 3- ), and phosphate (PO 43- ). Chemosphere. Elsevier Ltd; 2015;119:646–653.

Yuh-Shan H. Citation review of Lagergren kinetic rate equation on adsorption reactions. Scientometrics. 2004;59:171–177.

Zaini MAA, Okayama R, Machida M. Adsorption of aqueous metal ions on cattle-manure-compost based activated carbons. J Hazard Mater. 2009;170:1119–1124.

Zhang L, Xu S, Zhao W, Liu S. Co-pyrolysis of biomass and coal in a free fall reactor. Fuel. 2007;86:353–359.

Zhang M, Gao B, Yao Y, Xue Y, Inyang M. Synthesis of porous MgO-biochar nanocomposites for removal of phosphate and nitrate from aqueous solutions. Chem Eng J. Elsevier B.V.; 2012;210:26–32.

Zhao L, Cao X, Mašek O, Zimmerman A. Heterogeneity of biochar properties as a function of feedstock sources and production temperatures. J Hazard Mater. Elsevier; 2013;256:1–9.

Zheng H, Wang Z, Deng X, Herbert S, Xing B. Impacts of adding biochar on nitrogen retention and bioavailability in agricultural soil. Geoderma. Elsevier; 2013;206:32–39.

SUPPLEMENTARY MATERIAL

**Table 1.** Mean of total contents of BC, ZnBC, AlBC and FeBC.

| Materials | P | K | Ca | Mg | S | Fe | Zn | Al | Ni | Si |
|---|---|---|---|---|---|---|---|---|---|---|
| | ---------- g kg $^{-1}$ ---------- | | | | | | | | | |
| BC | 1.26 | 2.87 | 1.53 | 0.67 | 0.86 | 2.35 | 0.94 | 0.66 | 0.28 | 0.55 |
| ZnBC | 1.07 | 2.35 | 0.00 | 0.50 | 0.89 | 10.99 | 49.59 | 2.69 | 1.41 | 0.60 |
| FeBC | 1.19 | 1.71 | 0.00 | 0.00 | 0.92 | 62.34 | 0.19 | 6.42 | 0.16 | 0.57 |
| AlBC | 0.85 | 2.76 | 0.01 | 0.00 | 0.64 | 0.94 | 0.0 | 100.11 | 0.18 | 0.59 |

# Performance of biochar and humic acid as additives for soluble phosphate fertilizer

# Performance of biochar and humic acid for additives in soluble phosphate fertilizer

Maurício Cunha Almeida Leite[a], Edson Marcio Mattiello[a], Leonardus Vergtz[a], Wedisson Oliveira Santos[a], Fabiane Carvalho Ballotin[a], Patrícia Matias Cardoso[a].

[a] Department of Soil Science, Universidade Federal de Viçosa, Viçosa, Brazil.

ABSTRACT

Phosphate fertilization has low agronomic efficiency in clay tropical soils rich in Fe and Al oxyhydroxides due to the high orthophosphate chemisorption capacity of these adsorbents. Therefore, the use of coating substances in fertilizers capable of preventing the chemical adsorption of P in the soil can be strategic to increase the efficiency of these products. In this sense, the present work aims to evaluate the use of humic acid (HA) and chemically activated biochar (ZnBC) as additives in granules of monoammonium phosphate (MAP), as well as to study P diffusivity, P release and the growth of plants. Samples of ZnBC and HA were initially characterized as chemical composition and constituent elements. The diffusivity trials was performed using granules of MAP coated with HA (MAPHA) and ZnBC (MAPZnBC) in different coating ratios (0.5, 1 and 2%) in the granulesphere soil region. The P-soil release trial was evaluated by a stirred-flow system for MAPHA (1 %) and MAPZnBC (1 %) incubated in a clay soil. In order to evaluate the agronomic efficiency of MAPHA and MAPZnBC, an experiment was carried out under greenhouse conditions in clay soil using maize and soybean as plant tests. The P content of the shoots were evaluated, as well the dry matter and P uptake. The use of HA and ZnBC did not effectively affect the diffusivity of MAP granules. However, the MAPHA and MAPZnBC provided greater P release in the granulesphere by the P-soil desorption. It was observed that the results obtained by the P-soil trial were not translated with the same magnitude when the dry matter and P uptake parameters were evaluated, but the total P uptake of the two cycles was higher for the MAPHA treatment. It is concluded that ZnBC and HA have positive effects as an additive in terms of P-soil release, but only the MAPHA treatment had a positive response to P uptake by plants.

**Keywords:** Humic acid, activated biochar, coating fertilizer, phosphorus, adsorption, desorption.

# INTRODUCTION

The use of phosphorus fertilizers has been increasing significantly over the last decades in Brazil (Lu e Tian, 2017), having a substantial contribution to the green revolution in the country. Nonetheless, the amount of phosphorus (P) applied as fertilizer in soils is much higher than crop demand (Withers et al., 2018) due to the high P-adsorbing capacity of tropical soils, especially clay soils rich in Fe and Al oxi(hydroxides) (Novais e Smyth, 1999).

The reduction of the interaction of orthophosphate ions with the oxidic matrix of soil appears to be a possibility to increase the efficiency of phosphorus fertilization in highly weathered soils. On the perspective, the beneficial effect of adding organic materials to soil on the reduction of P adsorption is well known (Fink et al., 2016). Another promising strategy is the use of technologies linked to fertilizers, which P-protecting and increase its availability to plants (Benício et al., 2017).

Biochar (BC) and humic acid (HA) are example of organic materials that can be used as fertilizers coating to reduce the contact between orthophosphate ions and soil. Biochar is a product obtained from the thermal degradation of organic wastes under minimal oxygen conditions (Lehmann, 2014). In addition, this solid product can be activated and potentiate its physicochemical features such as surface area, charge density and adsorption capacity (Angin et al., 2013; Say e Güzel, 2016). Zinc chloride ($ZnCl_2$) has been widely used as an activator and co-pyrolysis agent to BC synthesis (Hayashi et al., 2002), in addition provide Zn that is an important nutrient for plants.

Humic acid can compete for adsorption sites of P by conditioner sorption that occurs in soil through the action of molecules able to compete with P through sites, covering clay minerals, reducing the area of these adsorbents or creating new adsorption sites (Borggaard et al., 1990; Gerke, 2010; Kleber et al., 2015; Fink et al., 2016).

In this context, we hypothesized that the use of organic additives as coatings of soluble phosphorus fertilizer has strong potential to interact with the surface of the granule, as well as the region to its surroundings and decreasing the sorption of P by Fe and Al oxyhydroxides. Thus, we aimed to evaluate the performance of soluble phosphate fertilizer coated with organic additives, such as activated BC and HA. Specifically, we assessed the P-diffusivity in soil, P-availability in the region surrounding the granule and the efficiency of recovery of P by plants in successive cultivation.

## MATERIALS AND METHODS

### *Soils*

The characterization the crystalline phases of the soils (supplementary material Figure S1) were accomplished by X-ray diffraction (XRD) analyses performed in a Shimadzu XRD-6000 diffractometer, using a graphite crystal monochromator to select Co-Kα1 radiation with λ = 1.5406 Å and a step way of 0.02°/s, with 2θ angle between 4° and 70°.

### *Biochar and humic acid production*

Sawdust (*Eucalyptus spp.*) (< 30 mm) was dried in closed circulation oven at 105° C until constant weight. After drying, 200 g of sawdust were added in 1 L of $ZnCl_2$ solution (204 g $L^{-1}$ of $ZnCl_2$) (sawdust:$ZnCl_2$ ratio mass of ~ 1:1). This suspension was stirred at 80 °C for 7 h, and then dried at a heating plate (200 °C) until the liquid evaporates. The sawdust impregnated with $ZnCl_2$ was again dried in a closed circulation oven at 105 °C until constant weight. This material was pyrolysed at 500 °C by 1 h and the heating rate was of 10 °C $min^{-1}$. After the production of zinc-biochar (ZnBc), the material underwent dialysis (deionized water) until the pH and electrical conductivity remained constant. The final product was milled and passed in 80 mesh (177µm) and stored for physicochemical analysis. Lastly, humic acid (HA) was extracted from leonardite (Alberta, Canada) by alkaline extraction (KOH) as a commercial product by fertilizer company.

### *Coating of granules*

We used monoammonium phosphate granules (MAP) (32 ± 2 mg) as a matrix for coating, which was dried at 50 °C to constant weight. A solution containing water, acetone, agglutinator (mucilage) and ZnBC or HA was pulverized on MAP granules, which were placed in an inclined rotative granulator (45°). To ensure that the bulk addition of the granules was due to the adherent solid materials and not to the moisture of the applied solution, an industrial dryer was used to remove excess moisture. The coating process was repeated until the final product had 0.5, 1.0 and 2.0 % (weight base) of additive (ZnBC or HA). At the end of the process, the fertilizers obtained were

MAPHA (MAP coated with HA) and MAPZnBC (MAP coated with ZnBC) with the coating ratios 0.5, 1 and 2 %. Lastly, morphology of granules coated with ZnBC and HA was analyzed by scanning electron microscopy (MEV) (Jeol model JSM 6010-LA).

*Materials characterization*

The total elements contents of HA were extracted by a nitroperchloric digestion ($HClO_4$: $HNO_3$ ratio of 1:4) and measured by Inductively Coupled Plasma Optical Emission Spectrometry (ICP-OES) (Table 2). Additionally, Total P, water-soluble P (water-P), and neutral ammonium citrate soluble P + water (NAC-P) in the fertilizers were measured as described by the Brazilian Ministry of Agriculture (Table 2). To assess the total element content of biochar was performed the digestion described by Enders and Lehmann (2012), followed by ICP-OES determination. Electrical conductivity (EC) and pH (Table 2) of the suspension in water was performed considering the ratio 1:20 (m / v), after intermittent shaking (90 rpm) for 24 h (Zhao et al., 2013).

The specific surface area (SSA) of ZnBC was estimated by adsorption of N2 at 77 K (Quantachrome, model NOVA 2200e) by the BET model (Brunauer et al., 1938) (P / P0 between 0.05-0.25). The samples under analysis were prepared as described by ASTM (2012). The porous volume was estimated by the BJH model (Barrett et al., 1951) in the range 0.99-0.60 relative pressure on the desorption isotherm. Data were processed by NOVAWin software.

A qualitative investigation of functional groups of HA and ZnBC was performed by attenuated total reflectance Fourier transform infrared spectroscopy (ATR- FTIR) (Jasco spectrometer, model FT/IR-4100), spectra were collected at wavenumber range of 4000 to 500 $cm^{-1}$ with a resolution of 4 $cm^{-1}$ and 256 scans.

*P-diffusivity trial*

A Petri dish (850 × 10 mm) trial was performed to evaluate the P-diffusivity in region around of the granule, which we called granulesphere soil. Double factorial scheme plus two additional treatments in completely randomized design with four replications was adopted [1 + 1 (2 x 3)]. As additional treatments, non-fertilized petri dish and control treatment (MAP).We used two soils (Table 1) of contrasting textures

(sandy and clayey soil) and three coating ratios (0.5, 1 and 2 %) for MAPZnBC and MAPHA. P-diffusivity was evaluated at 1 and 20 d of incubation. Therefore, 55 $cm^3$ of air-dried soil was placed in Petri dishes, ensuring a flat soil surface. A single granule of each treatment (32 mg ± 0.02) was placed at 0.3 cm of depth in the middle of the Petri dish, and the soil moisture was raised to 80% of soil field capacity. Then, Petri dishes were sealed with parafilm in order to minimize water losses and incubated at 25 °C.

The P-diffusivity was evaluated through of indicator filters paper placed on humid soil surface, which become green upon contact with the soil region where there was P-diffusivity (Degryse e McLaughlin, 2014). After this process, the filter papers were dried and the green area measured by images scanned and processed using imaging software (GNU Image Manipulation Program, v. 2.6.11). The effective radius of diffusion (ERD) was calculated through Equation 1.

$$ERD(mm)=\sqrt{Ap/\pi} \quad \text{(Eq. 1)}$$

where Ap ($mm^2$) is the green area colored by P.

**Table 1** Chemical and physical properties of the soils (top layer 0-30 cm) after liming.

| Soil | pH | OM | P | S | $K^+$ | Zn | $Mg^{2+}$ | $Ca^{2+}$ | H+Al | SB | T | V | Rem-P |
|---|---|---|---|---|---|---|---|---|---|---|---|---|---|
| | $H_2O$ | g $kg^{-1}$ | --------- mg $dm^{-3}$ -------- | | | | ---------- $cmol_c$ $dm^{-3}$ ---------- | | | | | % | mg $L^{-1}$ |
| Clay | 6,00 | 10,6 | 0,4 | 10,5 | 10,00 | 0,44 | 0,35 | 1,23 | 1,3 | 1,61 | 2,91 | 55,3 | 10 |
| Sand | 6,20 | 14,6 | 0,4 | 33,6 | 2,00 | 0,70 | 0,66 | 2,94 | 0,5 | 3,61 | 4,11 | 87,8 | 30 |

| | Clay | Silt | Coarse sand | Fine sand |
|---|---|---|---|---|
| | ---------- kg $kg^{-1}$ ---------- | | | |
| [1/]Clay | 0,799 | 0,008 | 0,104 | 0,089 |
| [2/]Sand | 0,272 | 0,014 | 0,240 | 0,474 |

M1 = available P extracted by Mehlich-1 solution; Rem-P = Remaining P; OM = organic matter. [1/]Clay <0.002 mm [2/]Sand 0.05 to 2 mm.

*P-soil release*

P-soil release trial was carried out on clayey soil (Table 3) to evaluate the P-availability in the granulesphere, allowing determining if the coatings would have an effect on P-availability. Therefore, a new Petri dish assay was performed, which was similar to the P-diffusivity trial. After 30 f of incubation, soil samples were collected using a ring with 1.00 cm of diameter, taking as reference the center where the fertilizer granule was applied. These samples were air-dried and underwent a P-desorption by a continuous flow system (1 ml $min^{-1}$). The system consists of reservoirs of solutions, piston pump (HPLC - Thermo Scientific, ultimate 3000), acrylic reactor (internal volume of 17 mL) mounted on magnetic stirrer (400 rpm) and automatic fraction collector (Gilson, FC 203B fraction collector) (Benício et al., 2017). Only samples (0.78 $cm^3$) of the treatments MAPHA (1 %), MAPZnBC (1 %), MAP and a non-fertilized soil were evaluated. Desorption was performed in triplicate using a solution of 10 µmol $L^{-1}$ of KCl and pH 6 (simulating the soil solution). The P contained in the fractions was measured by molecular absorption spectrometry (Braga, J. M, Defelipo, 1974). The P-recovery rate (PRR) was obtained from P-desorption over time (up to 100 min) (equation 2).

$$PRR(\%) = \left(\frac{\sum_{i=0}^{n} Des_i}{7.26}\right) \times 100 \qquad \text{(Eq. 2)}$$

Where ∑Des is sum of P desorbed at $time_i$ and 7.26 (mg) represent the P mass initial of the incubate granule.

*Greenhouse trial*

MAP agronomic performance was compared to fertilizers MAPBCZn 1% and MAPAH 1% in a pot experiment with sequential cultivations of maize and soybean on clayey soil (Table 3). Double factorial scheme plus an additional treatment in a block-randomized design with four replications was adopted [1 + (3 x 4)], as additional treatment a negative control (without P) was used. The factors: three P sources (MAP, MAPBcZn 1 % and MAPSH 1 %) and five P doses (100, 200, 300 and 400 mg $dm^{-3}$ of P). The fertilizer was mixed at pot center with a specific soil volume, using a cylinder that correspond to 30 % of the volume of the pot.

For the first crop, six seeds of maize (Biomatrix BM709 PR02) were sown per pot at 2 cm of depth. After seedling emergence, were selected two plants to maintain per pot A multi-element solution containing N, K, S, B, Zn, Cu, Mn and Mo was added at 10, 20, and 30 d after sowing, providing, 200 mg $dm^{-3}$ N, 150 mg $dm^{-3}$ K, 50 mg $dm^{-3}$ S, 1.21 mg $dm^{-3}$ B, 4.5 mg $dm^{-3}$ Zn, 1.3 mg $dm^{-3}$ Cu, 5.4 mg $dm^{-3}$ Mn and 0.15 mg $dm^{-3}$ Mo (Novais et al., 1991). Soil moisture was controlled daily to maintain at ~ 80% field capacity. After 35 d of grown, maize shoots were harvested at the soil surface. Plant tissues were oven-dried at 70 °C for 72 h (until constant weight), weighed and milled for chemical analysis. Afterwards, plant tissues were submitted to nitric-perchloric digestion (Embrapa, 2009) and P content was quantified by ICP-OES (Agilent, Series AA Model 240 FS)

Two days after maize harvesting, six seeds of soybean (M6210 IPRO) inoculated with *Bradyrhizobium* were sown into undisturbed soil pots at 2 cm of depth. After seedling emergence, only two plants were maintained per pot. A solution containing Zn, Cu, Mn and Mo were added at 10, 20 and 30 d after sowing, providing 4.5, 1.3, 5.4 and 0.15 mg $dm^{-3}$, respectively. After 48 d the shoots of the soybean were harvested by cutting the stems at the soil surface. Then, the same post-harvest procedure of maize was adopted.

*Statistical analysis*

Data of P-diffusivity trial were submitted to analysis of variance and means were compared using the Tuckey test ($p<0.05$). To greenhouse trial, identity test ($p<0.05$) was adopted on the regression models (Regazzi, 1999) that describe shoot dry matter mass, P uptake, total dry matter and total P uptake of maize and soybean as response to different sources and doses of P. The RStudio program (1.2.1335 version) and ExpDes package (Ferreira et al., 2013) were employed in data analysis.

## RESULTS

*Humic acid and biochar characterization*

The total contents of the materials can be observed in Table 2. Both HA and ZnBC present low P values, demonstrating that the effects observed by the treatments

during the evaluations do not stem from the P content of these materials. The ZnBC showed high Zn content as expected due to activation.

**Table 2.** Total contents of HA and ZnBC; MAP total P content and its soluble portion in water ($H_2O$) and neutral ammonium citrate plus water ($NAC+H_2O$) .

| Materials | P | K | Ca | Mg | S | Fe | Zn | Al | Ni | Si |
|---|---|---|---|---|---|---|---|---|---|---|
| | g kg$^{-1}$ | | | | | | | | | |
| HA | 1.35 | 67.40 | 10.50 | 1.41 | 4.37 | 4.08 | 0.01 | 10.27 | 0.00 | 0.00 |
| ZnBC | 1.07 | 2.35 | 0.00 | 0.50 | 0.89 | 10.99 | 49.59 | 2.69 | 1.41 | 0.60 |

| MAP | P-Total[1/] | P-NAC+$H_2O$[2/] | P-$H_2O$[3/] |
|---|---|---|---|
| | g kg$^{-1}$ | | |
| | 226.4 | 194.2 | 187.7 |

1/ nitroperchloric extraction; 2/ extraction in neutral ammonium citrate (pH 7); 3/ extraction in water, all described according to Brazilian Ministry of Agriculture, Livestock, and Food Supply, Normative Instruction No. 28 (Brasil, 2007).

The specific surface area (SSA) and total pore volume (TPV) are properties that can vary greatly depending on the type of biomass used in the synthesis, the rate of heating and pyrolysis temperature, including the type of chemical activation (Lehmann and Joseph, 2015; Tan et al., 2016). The Table 3 presents the results of pH, electric conductivity (EC), SSA and TPV for ZnBC. The values of SSA and VTP are in agreement with Yorgun et al., (2009); Altintig e Kirkil, (2016) and Xia et al., (2016) that also evaluated chemical activation of biochars with $ZnCl_2$.

**Table 3**. Resume of characteristics and properties of the activated ZnBC.

| pH | EC<br>µS | SSA<br>$m^2\ g^{-1}$ | TPV<br>$cm^3\ g^{-1}$ |
|---|---|---|---|
| 6.06 | 19.0 | 940 | 0.06 |

pH in water 1:20; Specific surface area BET-$N_2$ (SSA)(Brunauer et al., 1938), total pore volume (TPV) (Barrett et al., 1951).

The results for FTIR spectra ZnBC and HA are shown in figure 2. Absorption ATR-FTIR bands in the range between 3400 and 3200 $cm^{-1}$, with a peak at 3326 $cm^{-1}$, are typical of OH groups. Bands at 2912 and 2843 $cm^{-1}$ were assigned to aliphatic CH. The absorption bands at ~1620-1420 $cm^{-1}$ were assigned to an aromatic ring-like C=C stretching mode in polyaromatics. These results are in accordance with reported data (Ausavasukhi et al., 2016; Maluf et al., 2018).

For ZnBC there are common peaks characteristic of coal materials in the spectrum of BC, the band in 1685 $cm^{-1}$ is due to C=O stretching. Furthermore, in 1560 $cm^{-1}$ it was observed C=C stretching due to coal aromatic ring. and related to C-O stretching in 1157 $cm^{-1}$ (Liou, 2009) . Besides that, on ZnBC spectrum, a wide band in 3400 $cm^{-1}$ related to adsorbed water (OH groups stretching) was founded.

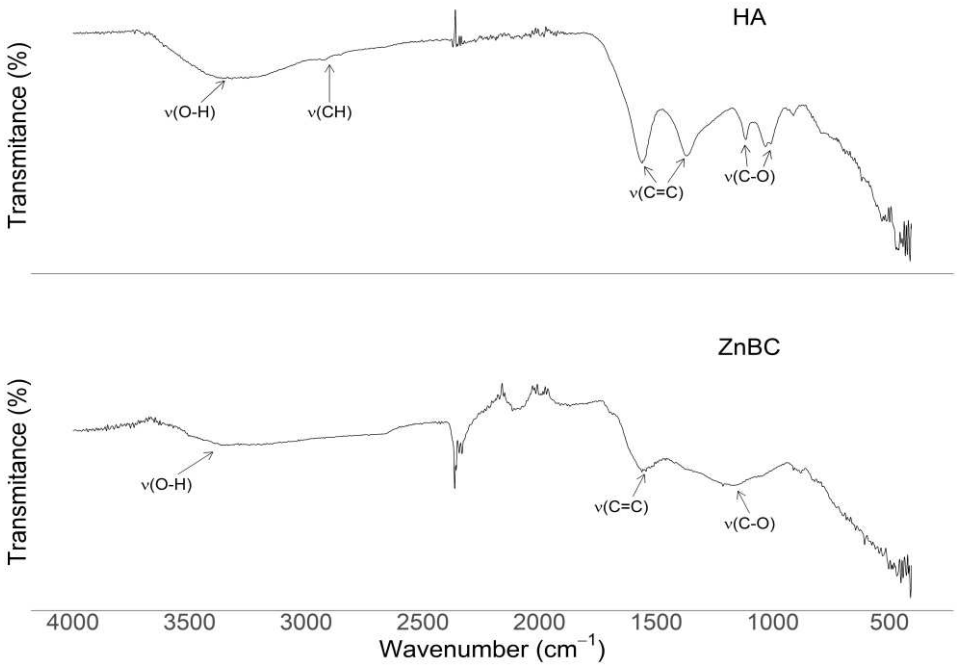


**Figure 2.** Infrared spectrum ZnBC and HA.

*Phosphorus diffusion assay*

The results of P diffusion using the filter paper technique are shown in figures 3 and 4. In general, the fertilizers showed similar patterns of P diffusion for each soil. Diffusion occurred rapidly for all treatments in the diffusion analysis 1 day after incubation. The sandy soil presented greater diffusivity in relation to the clayey soil as expected. The faster diffusion of P in sandy soil compared to clayey soil can be explained by the weaker P sorption in this soil (Degryse and McLaughlin, 2014). In the sandy soil, the diffusion of P fertilizer varied from 10.4 to 17.6 mm of effective diffusion radius (ERD) among the treatments. On the other hand, in clayey soil, the variation between fertilizers was 10.6 to 13.5 mm of ERD. The diffusion difference between the treatments in the two soils can be visualized in figures 3 and 5.

There was no difference for the sandy soil in 1 d of evaluation between MAP, MAPHA and MAPZnBC for any of the coating rates. At 20 d of incubation MAPHA and MAPZnBC coatings showed less diffusivity in relation to MAP, however no diference was observed between the different coating ratios. For clayey soil, there was no diference among the treatments and the coating ratios in 1 and 20 d of evaluation as observed in figures 2 and 2.1

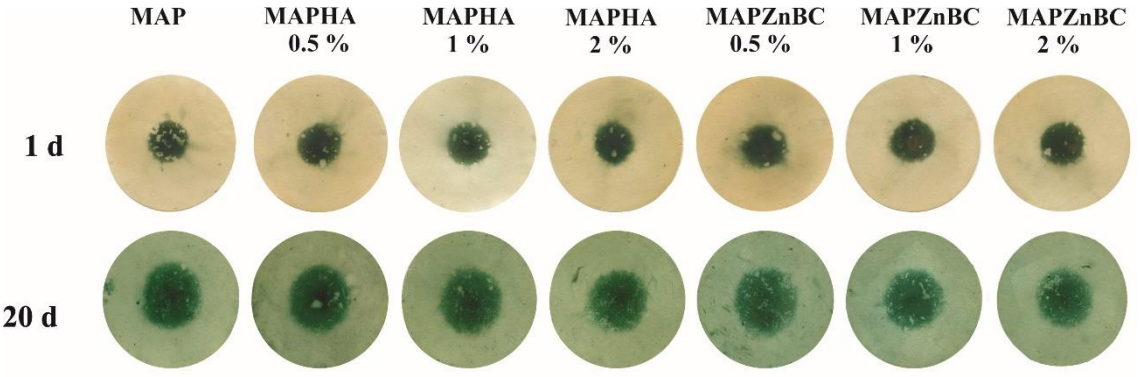


**Figure 2** Visualization of the diffusion zone of P at 1 and 20 d after addition of fertilizer granule and incubation at the sandy soil. Only one repetition is shown, since all repetitions present similar results.

**Figure 3.** Effective radius of diffusion (ERD) of sandy soil in 1 d and 20 d of incubation.

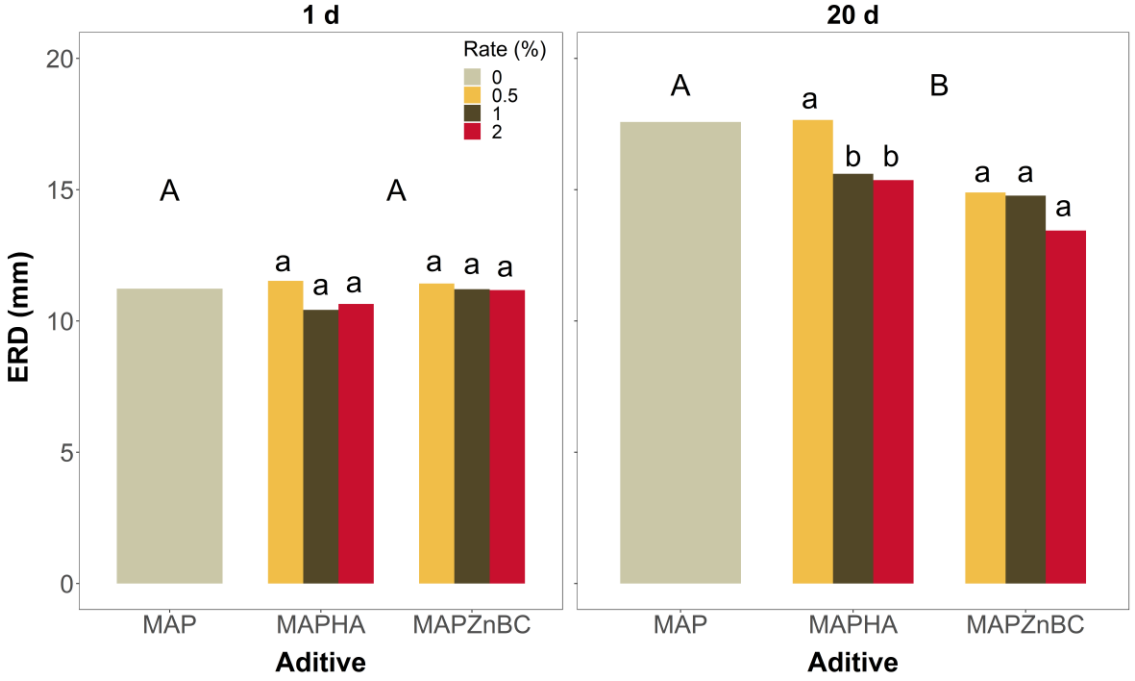


Columns with the same letters do not differ statistically (p <0.5) by the Tuckey test. (i) capital letters - comparison of different fertilizers at the same time of incubation.(ii) lowercase letters - comparison of different coating ratios within each treatment.

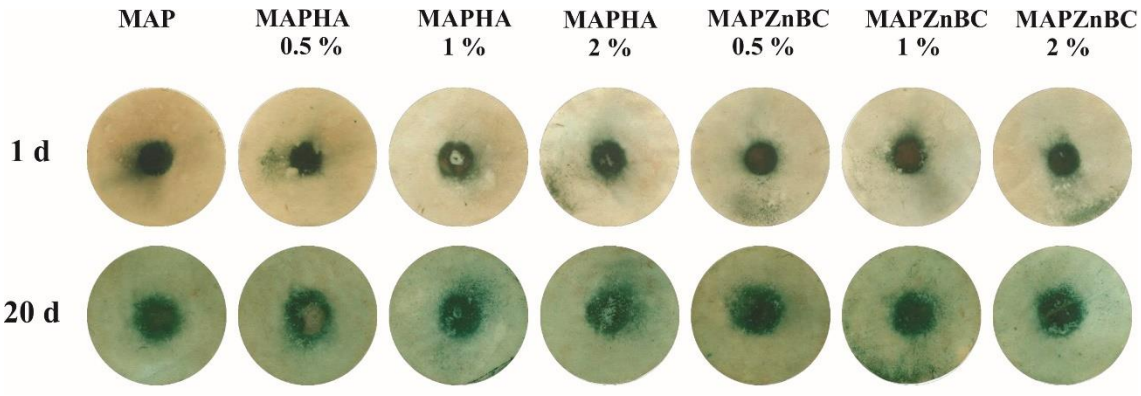


**Figure 4** Visualization of the diffusion zone of P at 1 and 20 d after addition of fertilizer granule and incubation at the clayey soil. Only one repetition is shown, since all repetitions present similar results.

**Figure 5.** Effective radius of diffusion (ERD) of a clayey soil in 1 d and 20 d of incubation.

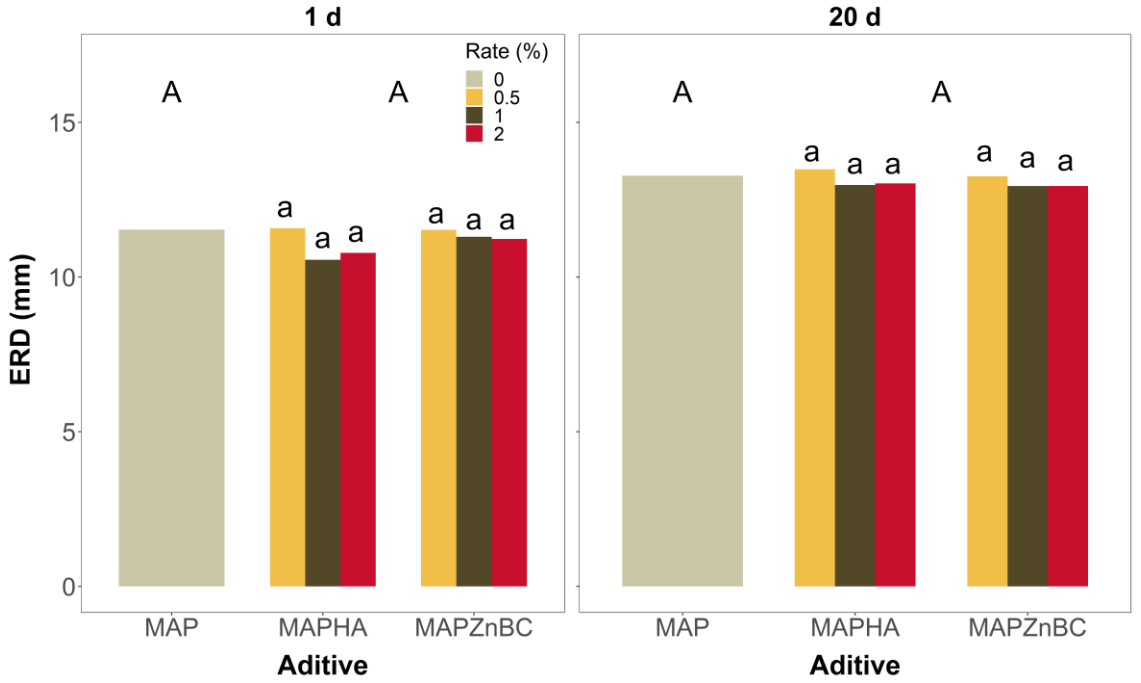


Columns with the same letters do not differ statistically (p <0.5) by the Tukey test (i) capital letters - comparison of different fertilizers at the same time of incubation.(ii) lowercase letters - comparison of different coating ratios within each treatment.

The results of accumulated desorption values are shown in figure 6. The treatments MAPHA (1%) and MAPZnBC (1%) demonstrated the ability to raise P availability in the region surrounding the granule. The sum of desorption corresponds to

the values obtained at each time point by desorption of the clay soil, in the region around the granule. These values express the ability of each coating to influence the phosphorus availability of the MAP granule.

The treatments with no significant differences in P diffusivity, both MAPHA and MAPZnBC, increased P availability in relation to the uncoated treatment (MAP) in the region surrounding the granule, even after 30 d of incubation.

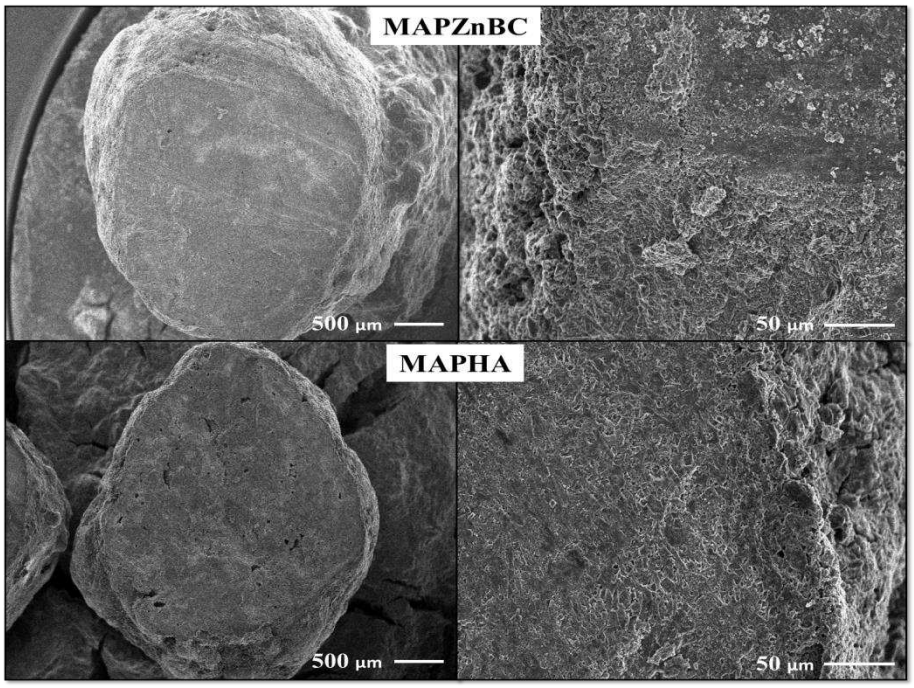


**Figure 6.** Scanning electron microscopy (SEM) of different coated surfaces: MAPZnBC (1 %) and MAPHA (1 %).

***P-soil release***

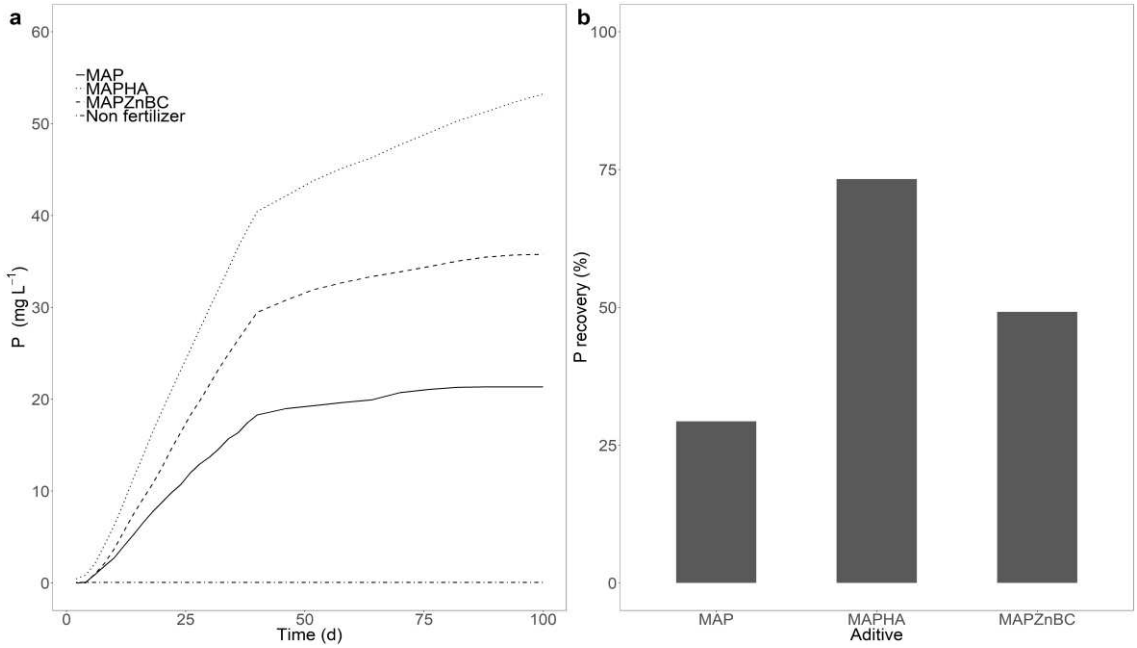


**Figure 6.** a: Sum values of P (mg $L^{-1}$) obtained by desorption of soil incubated 30 d in the clayey soil with MAPHA (1 %), MAPZnBC (1 %), MAP and a non-fertilized treatment. b: P recovery rate (%) of MAPHA, MAPZnBC and MAP.

Using the total value of the sum, that is, the value that expresses the total amount desorbed by water, an efficiency rate can be obtained for each treatment. The percentage differences can be seen in figure 6. The MAPHA, MAPZnBC and MAP treatments enabled 73, 49 and 29% respectively of total P recovery in the granulesphere to remain available in water after 30 d of incubation.

*Agronomic evaluation of coated phosphate fertilizers*

In general, it was observed a minor effect by the addition of organic additives in MAP (figure 8). The values of shoots dry matter (SDM) show that for maize cultivation, the MAPHA and MAPZnBC treatments had no significant difference when compared to the uncoated treatment (MAP). However, treatment with MAPZnBC showed a significant difference in relation to MAPHA treatment. In the second crop (soybean), the MAPZnBC treatment presented the lowest values of SDM, presenting significant difference between the MAP and MAPHA treatments. For cultivation with maize, the treatments MAP and MAPZnBC did not present a significant difference for P uptake contents. In the P uptake for maize, the treatments presented no significant difference

for the soybean when comparing the difference between the models by the identity test. However, for P uptake and total uptake (maize and soybean), the MAPHA treatment showed to be greater as compared with the other treatments, presenting a significant difference by the model identity test.

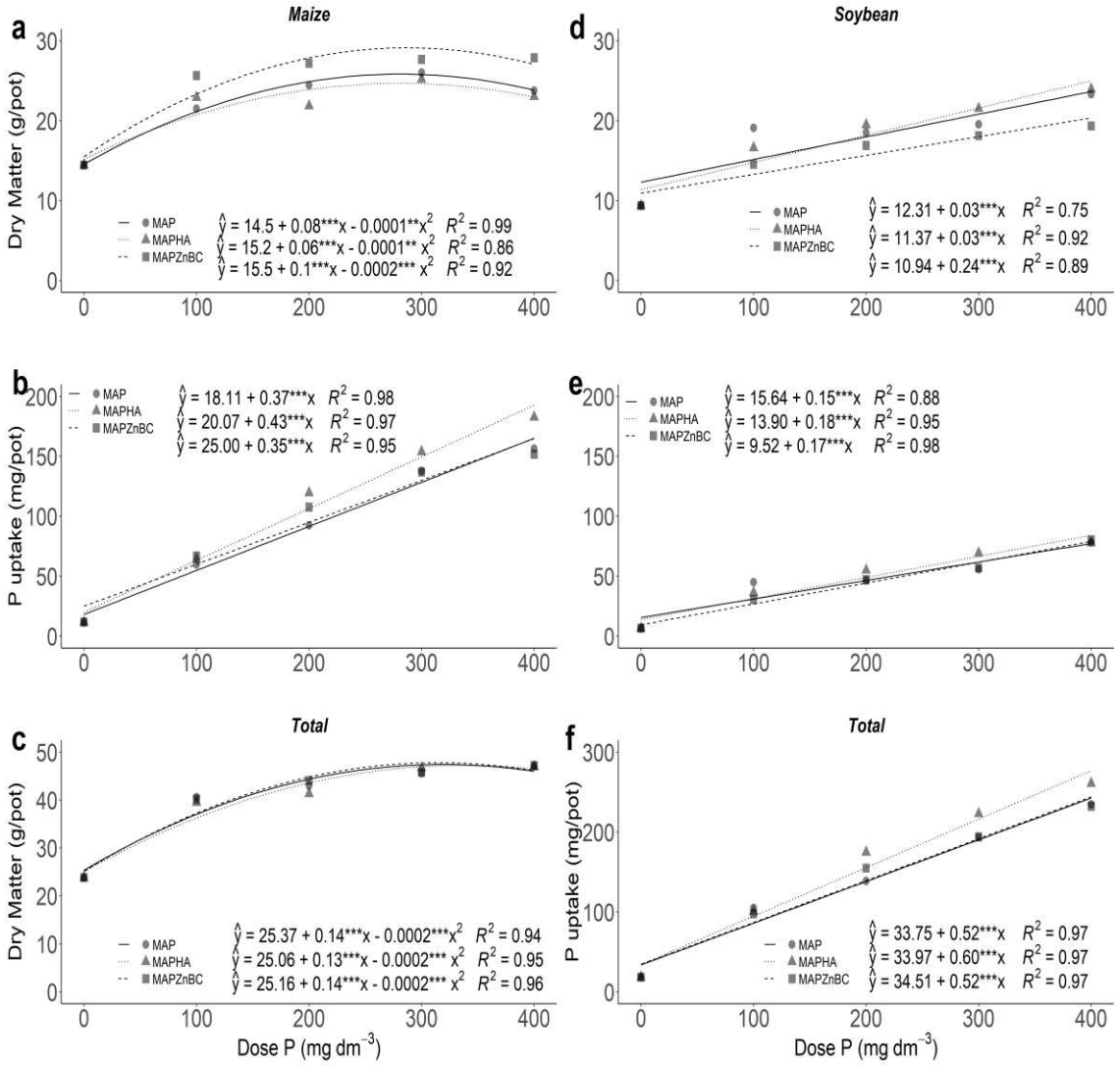


**Figure 7**. a- Maize dry matter yield, b- maize P uptake, c- total dry matter (maize and soybean), d- soybean dry matter yield, e- soybean P uptake and f- total P uptake (maize and soybean), as a function of doses and different additives MAP, MAPHA (1%) and MAPZnBC (1%).

The model identity test (table 4) shows that, for maize cultivation, the MAPZnBC treatment showed a difference of the other treatments in relation to SDM. As for the soybean, the treatment MAPZnBC had the lowest values of SDM for the doses of P evaluated. For the P uptake parameter, MAPZnBC treatment showed a

significant difference in relation to MAP and MAPZnBC for maize. In soybean, all treatments did not present significant difference, demonstrating equality. There was no significant difference between the SDM and the PMA models, but the MAPHA treatment showed a significant difference for the other treatments, demonstrating that the HA coated granules allowed a higher accumulation of P over the two crops.

**Table 4.** Comparison of the models of each parameter by the model identity test.

| Parameters | MAP *vs* MAPHA | MAP *vs* MAPZnBC | MAPHA *vs* MAPZnBC |
|---|---|---|---|
| | ---------- *p value* ---------- | | |
| | | Maize | |
| SDM | 0.88 | 0.06 | 0.01 |
| P uptake | 0.01 | 0.76 | 0.03 |
| | | Soybean | |
| SDM | 0.71 | 0.04 | 0.001 |
| P uptake | 0.55 | 0.52 | 0.37 |
| | | Total (maize + soybean) | |
| SDM | 0.94 | 0.98 | 0.83 |
| P uptake | 0.02 | 0.96 | 0.03 |

For values of p> 0.05 the models are statistically equal.

## DISCUSSION

### *Phosphorus diffusivity*

The main factors that affect diffusion are soil moisture, P maximum adsorption capacity and the amount of P added via fertilizer (Lehr et al. 1959). Due to this, it was expected that the additives could influence the P difusitivity by altering the kinetics and the interaction of P with soil. The HA treatments could act as a soil conditioner, acting on the interaction between the P and the oxyhydroxides surface, reducing the P adsorption (Fu et al., 2013). On the other side, it was expected that the use of ZnBC as an additive would have the opposite effect, reducing the diffusivity, due to the adsorptive characteristics of the activated biochar, acting as a matrix for the adsorption of P (Liang et al., 2006; Hunt et al., 2007). However, both coatings did not present an effective capacity to alter P difusivity.

From the point of view of reducing diffusivity, HA does not present good characteristics as granule protection. The HA is highly soluble at pH values above 2 (Mobed et. al 1996), which gives a rapid dissolution of the HA coating at pH (pH ± 6) and soil moisture (80 %) as of the present study. By the aspect of increasing P diffusivity, the HA could be able to decrease the adsorption of P by the surface of the oxides, due the interaction effects the HA and P, besides the interaction with the surface of the oxides . However these effects were not able to increase P diffusivity. For ZnBC, although it is a highly resistant structure, the hydrophobicity and the surface structure can influence its ability to protect MAP against water imbibition. According to Kinney et al., (2012), the 3000-2800 peak area (alkyl peak) was strongly correlated with hydrophobicity. However, these functionalities are destroyed by pyrolysis at temperatures between 400 °C and 500°C (Chen et al., 2008; Keiluweit et al., 2010), as showed for ZnBC, with a slope in the alkaline region of the material (figure 2). Another feature is the way in which the coating is formed, not allowing formation of a smooth and homogeneous surface around the granules, existing cracks and hollows in this structure in MAPZnBC (figure 5). Both coatings have weak points in terms of increasing diffusivity or acting as a slow diffusion coating, not being able to change the diffusitivity effectively. This is probably the reason why the coated treatments presented similar values to the uncoated treatment (MAP) in terms of diffusion.

However, less diffusivity can not necessarily be interpreted as less availability of P. For example, McBeath et al. (2012), evaluated P and Zndispone availabilityfertilizers, applied to dry and moist soil, with 80 % of field capacity. The authors verified that there was less diffusivity of P, but there were no changes in the P available values for the plants. These verifications are important to understand the role of the use of activated BC and HA as additives with the ability to change the kinetics of P in the granulesphere.

*P-soil release*

Considering the granulesphere soil, we observed that the treatments MAPHA (1 %) and MAPZnBC (1 %) showed higher availability of P in water, as shown in figure 4 and 5. As HA are an important component of humic substances (Antelo et al., 2007), the results of P desorption and recovery rate are in agreement with data from (Fu et al., 2013; Wang et al., 2016), where these authors evaluated the affinity between phosphates ($H_2PO_4^-$, $HPO_4^{2-}$), oxyhydroxides and HA observing a positive effect of these materials

on the decrease of P sorption in Fe and Al hydroxides. The reported effects of HA and organic anion on the interaction of the phosphate anion with the surface of the clay minerals are reported as different mechanisms such as action of organic molecules that compete with P for binding sites, decreasing goethite and hematite specific surface area able to adsorb P (Wang et al., 2016), modification of the interaction of the P with the surface by the change of surface charges, dissolution of adsorbents, or by the creation of new adsorption sites (Borggaard et al., 1990; Gerke, 2010; Hinsinger et al., 2011). However, Borggaard et al., (2005) observed little influence of addition of humic substances in concentrations comparable to naturally occurring contents on the amount of phosphate adsorbed by synthetic aluminum oxide, ferrihydrite and goethite. These results demonstrate that the concentration, type of organic source and the evaluation method used can influence the effects in the organic compounds on the kinetics of P.

The treatment MAPZnBC also presented higher values for P recovery in granulesphere soil compare to MAP in the desorption test. In the soil, there is a competition between the mineral soil sorption complex and biochar (Morales et al., 2013), once it can alters P availability through its anion exchange capacity (Cui et al., 2011,). This effect is expected due to the process of chemical activation of the material as the ZnBC, which generates charges on the surface of the material, besides increasing the specific surface area and pore volume (Table 2), due to the effect of $ZnCl_2$ in the co-pyrolysis process. As pointed out by Wang et al., (2017), the pyrolysis process generated Zn oxides, which may contribute to increase the surface area, once causes the enlargement of the pore structure by the metal oxide particles entering into the pores (Zaini et al., 2009).

In the present study, the analyses of P availability by the desorption assay in a continuous stirred-flow system has the advantages of being a sensitive evaluation, since the data are generated from the region with the greatest effect of the *treatments*, the granulesphere soil. The continuous flow evaluation also allows to generate data every minute, in a system in which the solution is constantly replenished, maintaining the balance between the solution and the soil in a constant way over time (Guedes et al., 2016). Nevertheless, the results obtained in small scale analyzes may not be transcribed in the same proportion for evaluations at larger scales or evaluations with organisms such as plants.

*Agronomic evaluation*

In the greenhouse experiment, the treatment MAPZnBC presented higher SDM for the first corn crop. However, for P uptake, the MAPZnBC treatment did not present the same performance, presenting the lowest P recovery for soybean cultivation when compared to the others. Although the data obtained in the continuous flow desorption experiment showed that the soil incubated with MAPZnBC showed a 20% higher recovery rate of P in water during the evaluation time as compared to the MAP, this "recovery rate" may not be expressed in plant availability. Since ZnBC exhibits characteristics of acting as a matrix for the adsorption of P, due of the high surface area, it is not understood as the rate of desorption of P by biocharine aligns the needs of absorption by plants.

On the other hand, P uptake values demonstrated that the MAPHA treatment increase the P availability for the first crop with corn, which resulted in a higher total P uptake. These results are interesting because they demonstrate that the use of HA as an additive in phosphate fertilizers may increase P recovery rate, probably due to the effects of HA on interaction with soil and P kinetics (Morales et al., 2013) in the granulesphere soil. These results are in agreement with the data observed by the stirred flow desorption trial (Figure 6), showing that the use of HA as an additive can increase the availability of P.

To better understand how each material affects the P availability for plants, it would be necessary to analyze the equilibrium between P adsorbed to ZnBC and soil solution during more evaluation time and even to evaluate the P residue that remains in the biochar, even after incubating in soil. Although, the effects of HA on soil P availability are more widely studied, however, are dynamic. Therefore, study the speed that the reactions occur, and the time of permanence of these effects in the soil becomes an important point.

## CONCLUSIONS

In summary, the above discussion shows that the use of ZnBC and HA as additives in soluble phosphate fertilizer is not able to effectively change the diffusivity of the MAP. By means of more sensitive and small scale analyzes, the desorption evaluation showed that there is potential in these materials as additives that allow to increase the P availability on granulesphere soil, with emphasis on HA, which presented the highest

percentage of availability. However, the MAPZnBC treatment did not present the expected performance, not being able to increase the P availability for plants. On the other hand, the MAPHA treatment presented potential in both evaluations, promoting a higher soluble P value over the evaluated time in P-soil desorption kinetics and in the total P uptake values by the cultures. In the course of this study, it is possible to realize that methods that seek to evaluate in a sensible way small regions like the granulesphere soil are tools to select materials with greater positive potential.

*Acknowledgment*

The authors gratefully acknowledge funding received from Conselho Nacional de Desenvolvimento Científico e Tecnológico (CNPq) and Fertilizantes Heringer.

REFERENCES

Altintig E, Kirkil S. Preparation and properties of Ag-coated activated carbon nanocomposites produced from wild chestnut shell by ZnCl2 activation. J Taiwan Inst Chem Eng. Elsevier B.V.; 2016;63:180–188.

Angin D, Altintig E, Köse TE. Influence of process parameters on the surface and chemical properties of activated carbon obtained from biochar by chemical activation. Bioresour Technol. Elsevier Ltd; 2013;148:542–549.

Antelo J, Arce F, Avena M, Fiol S, López R, Macías F. Adsorption of a soil humic acid at the surface of goethite and its competitive interaction with phosphate. Geoderma. 2007;138:12–19.

ASTM - American Society for Testing and Materials. D6556 - 10 -Standard Test Method for Carbon Black — Total and External Surface Area by Nitrogen Adsorption. In: Annual Book of ASTM Standards, 2012.

Ausavasukhi A, Kampoosaen C, Kengnok O. Adsorption characteristics of Congo red on carbonized leonardite. J Clean Prod. Elsevier Ltd; 2016;134:506–514.

Barrett EP, Joyner LG, Halenda PP. The determination of pore volume and area distributions in porous substances. I. Computations from nitrogen isotherms. J Am Chem Soc. ACS Publications; 1951;73:373–380.

Benício LPF, Constantino VRL, Pinto FG, Vergütz L, Tronto J, Da Costa LM. Layered

Double Hydroxides: New Technology in Phosphate Fertilizers Based on Nanostructured Materials. ACS Sustain Chem Eng. 2017;5:399–409.

Borggaard OK, Jdrgensen SS, Moberg JP, Rabenlange B. Influence of organic matter on phosphate adsorption by aluminium and iron oxides in sandy soils. J Soil Sci. 1990;41:443–449.

Borggaard OK, Raben-Lange B, Gimsing AL, Strobel BW. Influence of humic substances on phosphate adsorption by aluminium and iron oxides. Geoderma. 2005;127:270–279.

Braga, J. M.; Defelipo, B. Determinação espectrofotométrica de fósforo em extratos de solo e material Vegetal. Revista Ceres, v. 21, p. 73−85, 1974.

Brasil. Ministério da Agricultura, Pecuária e Abastecimento. Instrução normativa n° 28, de 27 de Julho de 2007. Aprovar os Métodos Analíticos Ofciais para Fertilizantes Minerais, Orgânicos, Organo-Minerais e Corretivos, disponíveis na Coordenação-Geral de Apoio Laboratorial - CGAL/SDA/MAPA, na Biblioteca Nacional de Agricultura - BINAGRI e no sítio do Ministério da Agricultura, Pecuária e Abastecimento na rede mundial de computadores, endereço eletrônico: www.agricultura.gov.br. Brasília, DF: Diário Oficial da União; 2007. p. 11.

Brunauer S, Emmett PH, Teller E. Adsorption of gases in multimolecular layers. J Am Chem Soc. ACS Publications; 1938;60:309–319.

Chen B, Zhou D, Zhu L. Transitional adsorption and partition of nonpolar and polar aromatic contaminants by biochars of pine needles with different pyrolytic temperatures. Environ Sci Technol. 2008;42:5137–5143.

Cui H-J, Kuang Wang M, Fu M-L, Ci E. Soils, Sec 1 • Soil organic matter dynamics and nutrient cycling • Enhancing phosphorus availability in phosphorus-fertilized zones by reducing phosphate adsorbed on ferrihydrite using rice straw-derived biochar.

Degryse F, McLaughlin MJ. Phosphorus Diffusion from Fertilizer: Visualization, Chemical Measurements, and Modeling. Soil Sci Soc Am J. The Soil Science Society of America, Inc.; 2014;78:832.

EMBRAPA. Manual de análises químicas de solos, plantas e fertilizantes. Rio de Janeiro: Embrapa Solos.: Embrapa Informação Tecnológica, 2009.

Enders A, Lehmann J. Comparison of Wet-Digestion and Dry-Ashing Methods for Total Elemental Analysis of Biochar. Commun Soil Sci Plant Anal. 2012;43:1042–1052.

Ferreira EB, Cavalcanti PP, Nogueira DA. ExpDes.pt: Experimental Designs pacakge (Portuguese). R package version 1.1.2. 2013;2952–2958.

Fink, Jessé R, Inda AV, Tiecher T, Barrón V. Iron oxides and organic matter on soil phosphorus availability. Cienc e Agrotecnologia. 2016;40:369–379.

Fink JR, Inda AV, Tiecher T, Barrón V. Iron oxides and organic matter on soil phosphorus availability. Ciência e Agrotecnologia. 2016;40:369–379.

Fu Z, Wu F, Song K, Lin Y, Bai Y, Zhu Y, Giesy JP. Competitive interaction between soil-derived humic acid and phosphate on goethite. Appl Geochemistry. Elsevier Ltd; 2013;36:125–131.

Gerke J. Humic (organic matter)-Al(Fe)-phosphate complexes: An underestimated phosphate form in soils and source of plant-available phosphate. Soil Sci. 2010;175:417–425.

Guedes RS, Melo LCA, Vergütz L, Rodríguez-Vila A, Covelo EF, Fernandes AR. Adsorption and desorption kinetics and phosphorus hysteresis in highly weathered soil by stirred flow chamber experiments. Soil Tillage Res. Elsevier B.V.; 2016;162:46–54.

Hayashi J, Horikawa T, Takeda I, Muroyama K, Nasir Ani F. Preparing activated carbon from various nutshells by chemical activation with K 2 CO 3. Carbon N Y. 2002;40:2381–2386.

Hinsinger P, Brauman A, Devau N, Gérard F, Jourdan C, Laclau JP, Le Cadre E, Jaillard B, Plassard C. Acquisition of phosphorus and other poorly mobile nutrients by roots. Where do plant nutrition models fail? Plant Soil. 2011;348:29–61.

Hunt JF, Ohno T, He Z, Honeycutt CW, Dail DB. Inhibition of phosphorus sorption to goethite, gibbsite, and kaolin by fresh and decomposed organic matter. Biol Fertil Soils. 2007;44:277–288.

Keiluweit M, Nico PS, Johnson MG. Dynamic Molecular Structure of Plant Biomass-derived Black Carbon(Biochar)- Supporting Information -. 2010;44:1–19.

Kinney TJ, Masiello CA, Dugan B, Hockaday WC, Dean MR, Zygourakis K, Barnes RT. Hydrologic properties of biochars produced at different temperatures. Biomass and

Bioenergy. Elsevier Ltd; 2012;41:34–43.

Kleber M, Eusterhues K, Keiluweit M, Mikutta C, Mikutta R, Nico PS. Mineral-Organic Associations: Formation, Properties, and Relevance in Soil Environments [Internet]. Adv. Agron. Elsevier Ltd; 2015.

Lehmann J. Biochar for Environmental Management. Biochar Environ. Manag. Routledge; 2014.

Lehmann J, Joseph S. Biochar for Environmental Management. Biochar Environ. Manag. 2015.

Liang B, Lehmann J, Solomon D, Kinyangi J, Grossman J, O'Neill B, Skjemstad JO, Thies J, Luizão FJ, Petersen J, Neves EG. Black Carbon Increases Cation Exchange Capacity in Soils. Soil Sci Soc Am J. 2006;70:1719.

Liou T-H. Development of mesoporous structure and high adsorption capacity of biomass-based activated carbon by phosphoric acid and zinc chloride activation. Chem Eng J. Elsevier; 2009;158:129–142.

Lu C, Tian H. Global nitrogen and phosphorus fertilizer use for agriculture production in the past half century: shifted hot spots and nutrient imbalance. Earth Syst Sci Data. 2017;9:181–192.

Maluf HJGM, Silva CA, Curi N, Norton LD, Rosa SD. Adsorption and availability of phosphorus in response to humic acid rates in soils limed with CACO3 or MGCO3. Cienc e Agrotecnologia. 2018;42:7–20.

McBeath TM, McLaughlin MJ, Kirby JK, Armstrong RD. Dry Soil Reduces Fertilizer Phosphorus and Zinc Diffusion but Not Bioavailability. Soil Sci Soc Am J. 2012;76:1301.

Mobed et. al 1996. Fluorescence Characterization of IHSS Humic Substances : Total Luminescence Spectra with Absorbance Correction. Environ Sci Technol. 2000;30:3061–3065.

Morales MM, Comerford N, Guerrini IA, Falcão NPS, Reeves JB. Sorption and desorption of phosphate on biochar and biochar-soil mixtures. Soil Use Manag. John Wiley & Sons, Ltd (10.1111); 2013;29:306–314.

Novais, R.F.; Neves, J.C.L. & Barros, N.F. Ensaio em ambiente controlado. In: Oliveira, A.J.; Garrido, W.E.; Araújo, J.D. & Lourenço, S., eds. Métodos de pesquisa em fertilidade do solo. Brasília, Embrapa-SEA, 1991. p.189-254.

Novais, R.F. & Smyth, T.J. Fósforo em solo e planta em condições tropicais. Universidade Federal de Vicosa, Vicosa, MG (Brasil). Dept. de Solos, 1999.

Regazzi AJ. Teste para verificar a identidade de modelos de regressão e a igualdade de parâmetros no caso de dados de delineamentos experimentais. Ceres. 1999;46:383–409.

Santos WO, Mattiello EM, Barreto MSC, Cantarutti RB. Acid Ammonium Citrate as P Extractor for Fertilizers of Varying Solubility. Rev Bras Ciência do Solo. 2018;43:1–12.

Say H, Güzel F. High surface area mesoporous activated carbon from tomato processing solid waste by zinc chloride activation: process optimization, characterization and dyes adsorption. J Clean Prod. 2016;113:995–1004.

Tan X, Liu Y, Gu Y, Xu Y, Zeng G, Hu X, Liu S, Wang X, Liu S, Li J. Biochar-based nano-composites for the decontamination of wastewater: a review. Bioresour Technol. Elsevier; 2016;212:318–333.

Wang H, Zhu J, Fu Q, Hong C, Hu H, Violante A. Phosphate adsorption on uncoated and humic acid-coated iron oxides. J Soils Sediments. Journal of Soils and Sediments; 2016;16:1911–1920.

Wang P, Tang L, Wei X, Zeng G, Zhou Y, Deng Y, Wang J, Xie Z, Fang W. Synthesis and application of iron and zinc doped biochar for removal of p-nitrophenol in wastewater and assessment of the influence of co-existed Pb(II). Appl Surf Sci. 2017;392:391–401.

Withers PJA, Rodrigues M, Soltangheisi A, De Carvalho TS, Guilherme LRG, Benites VDM, Gatiboni LC, De Sousa DMG, Nunes RDS, Rosolem CA, Andreote FD, Oliveira A De, Coutinho ELM, Pavinato PS. Transitions to sustainable management of phosphorus in Brazilian agriculture. Sci Rep. Springer US; 2018;8:1–13.

Xia D, Tan F, Zhang C, Jiang X, Chen Z, Li H, Zheng Y, Li Q, Wang Y. Applied Surface Science ZnCl 2 -activated biochar from biogas residue facilitates aqueous As ( III ) removal. Appl Surf Sci. 2016;377:361–369.

Yorgun S, Vural N, Demiral H. Preparation of high-surface area activated carbons from Paulownia wood by ZnCl2 activation. Microporous Mesoporous Mater. Elsevier Inc.; 2009;122:189–194.

Zaini MAA, Okayama R, Machida M. Adsorption of aqueous metal ions on cattle-manure-compost based activated carbons. J Hazard Mater. 2009;170:1119–1124.

Zhao L, Cao X, Mašek O, Zimmerman A. Heterogeneity of biochar properties as a

function of feedstock sources and production temperatures. J Hazard Mater. Elsevier; 2013;256:1–9.

SUPPLEMENTARY MATERIAL

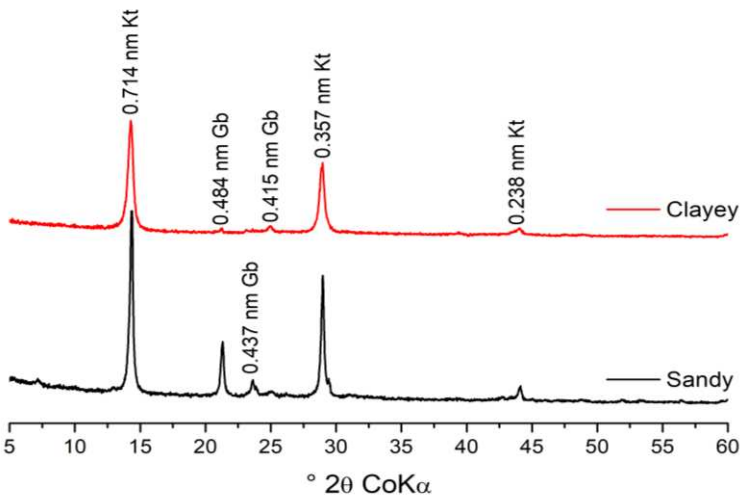


**Figure S1.** X-ray diffractograms of the clay fraction of the soils used (Kt = kaolinite and Gb = gibssite).

**Table S1**. Mean values of the diffusivity test for sand and clay soils.

| Sandy soil | | | | | | |
|---|---|---|---|---|---|---|
| Fertilizers | Coating ratio % | Incubation time of soil with fertilizer (d) | | | | |
| | | 1 | 5 | 12 | 20 | 32 |
| | | ---------- effective radius of diffusion (mm) ---------- | | | | |
| MAP | 0 | 11,2 | 14,2 | 17,1 a | 17,6 a | 14,1 a |
| MAPHA | 0,5 | 11,5 | 13,7 | 16,2 | 17,6 | 13,6 |
| | 1 | 10,4 | 12,6 | 16,9 | 15,6 | 11,8 |
| | 2 | 10,6 | 13,7 | 17,1 | 15,4 | 13,9 |
| MAPZnBC | 0,5 | 11,4 | 14,3 | 15,9 | 14,9 | 12,2 |
| | 1 | 11,2 | 13,3 | 15,5 | 14,8 | 11,8 |
| | 2 | 11,2 | 14,1 | 15,4 | 13,4 | 12,2 |
| Clayey soil | | | | | | |
| Fertilizers | Coating ratio % | Incubation time of soil with fertilizer (d) | | | | |
| | | 1 | 5 | 12 | 20 | 32 |
| | | ---------- effective radius of diffusion (mm) ---------- | | | | |
| MAP | 0 | 11,5 | 12,6 | 14,0 | 13,27 | 11,1 |
| MAPHA | 0,5 | 11,6 | 11,6 | 13,0 | 13,5 | 12,5 |
| | 1 | 11,0 | 11,3 | 12,5 | 13,0 | 10,7 |
| | 2 | 10,8 | 11,0 | 12,6 | 13,0 | 9,1 |
| MAPZnBC | 0,5 | 11,5 | 10,1 | 12,5 | 13.25 | 8,9 |
| | 1 | 11,3 | 9,7 | 12,7 | 12,9 | 8,1 |
| | 2 | 11,2 | 10,4 | 12,8 | 12.9 | 10,3 |

**Table S2**. Dry matter yield, content, content and recovery rate of P in maize, as a function of doses and different additives in MAP, MAPSH (1%); MAPZnBC (1%).

| Doses de P (mg $dm^{-3}$) | Fertilizers | | |
|---|---|---|---|
| | MAP | MAPHA | MAPZnBC |
| | | Shoots dry matter (g $pot^{-1}$) | |
| 0 | | 14.44 | |
| 100 | 21.49 | 22,90 | 25,65 |
| 200 | 24.45 | 21,86 | 27,19 |
| 300 | 26.02 | 25,18 | 27,66 |
| 400 | 23,77 | 23,01 | 27,87 |
| Mean fertilizers | 23,93 | 23,23 | 27,09 |
| | | Shoots P concentrate (g $kg^{-1}$) | |
| 0 | | 0.81 | |
| 100 | 2,85 | 2,85 | 2,62 |
| 200 | 3,79 | 5,52 | 3,98 |
| 300 | 5,30 | 6,20 | 4,95 |
| 400 | 5,89 | 8,09 | 5,58 |
| Mean fertilizers | 4,46 b | 5,66 a | 4,28 b |
| | | Shoots P uptake (mg $vase^{-1}$) | |
| 0 | | 11.66 | |
| 100 | 59,77 | 64,33 | 66,98 |
| 200 | 92,47 | 119,57 | 107,67 |
| 300 | 137,81 | 153,80 | 136,84 |
| 400 | 156,46 | 182,82 | 151,66 |
| Mean fertilizers | 111,63 | 130,13 | 115,79 |
| | | P recovery rate (%) | |
| 100 | 16,04 | 17,56 | 18,45 |
| 200 | 13,47 | 17,98 | 16,00 |
| 300 | 14,01 | 15,79 | 13,91 |
| 400 | 12,06 | 14,26 | 11,66 |
| Mean fertilizers | 13,90 | 16,40 | 15,01 |

**Table S3**. Dry matter yield, content, content and recovery rate of P in soybean, as a function of doses and different additives in MAP, MAPSH (1%); MAPZnBC (1%).

| Doses de P (mg $dm^{-3}$) | Fertilizers | | |
|---|---|---|---|
| | MAP | MAPHA | MAPZnBC |
| | | Shoots dry matter (g $pot^{-1}$) | |
| 0 | | 9.37 | |
| 100 | 19.10 | 16.60 | 14.52 |
| 200 | 18.54 | 19.47 | 16.89 |
| 300 | 19.55 | 21.52 | 18.12 |
| 400 | 23,32 | 23.94 | 19.34 |
| Mean fertilizers | 20.13 | 20.38 | 17.22 |
| | | Shoots P concentrate (g $kg^{-1}$) | |
| 0 | | 0.70 | |
| 100 | 2.37 | 2.18 | 2.08 |
| 200 | 2.51 | 2.84 | 2.79 |
| 300 | 2.87 | 3.18 | 3.14 |
| 400 | 3.36 | 3.26 | 4.12 |
| Mean fertilizers | 2.78 | 2.87 | 3.04 |
| | | Shoots P uptake (mg $vase^{-1}$) | |
| 0 | | 6.60 | |
| 100 | 45.14 | 36.26 | 30.55 |
| 200 | 46.43 | 55.03 | 47.11 |
| 300 | 55.96 | 69.38 | 56.91 |
| 400 | 78.31 | 77.87 | 80.42 |
| Mean fertilizers | 56.46 | 59.64 | 53.75 |
| | | P recovery rate (%) | |
| 100 | 12.84 | 9.88 | 7.98 |
| 200 | 6.64 | 8.07 | 6.75 |
| 300 | 5.48 | 6.97 | 5.59 |
| 400 | 5.97 | 5.93 | 6.15 |
| Mean fertilizers | 7.73 | 7.71 | 6.61 |

**Table S4.** Total dry matter yield, total content and total recovery rate of the two production cycles (maize and soybean) as a function of doses and different aditives in MAP, MAPHA (1%), MAPZnBC (1%).

| Doses de P (mg $dm^{-3}$) | Fertilizers | | |
|---|---|---|---|
| | MAP | MAPHA | MAPZnBC |
| | Total shoots dry matter (g $pot^{-1}$) | | |
| 0 | | 23.82 | |
| 100 | 40.59 | 39.49 | 40.17 |
| 200 | 42.99 | 41.33 | 44.08 |
| 300 | 45.58 | 46.69 | 45.78 |
| 400 | 47.09 | 46.94 | 47.21 |
| Mean fertilizers | 44.06 | 43.61 | 44.31 |
| | Total shoots P uptake (mg $vase^{-1}$) | | |
| 0 | | 18.26 | |
| 100 | 104.91 | 36.26 | 97.53 |
| 200 | 138.90 | 55.03 | 154.79 |
| 300 | 193.78 | 69.38 | 193.75 |
| 400 | 234.77 | 77.87 | 232.08 |
| Mean fertilizers | 168,09 | 189,77 | 169,54 |
| | Total P recovery rate (%) | | |
| 100 | 28.89 | 27.45 | 26.43 |
| 200 | 20.11 | 26.06 | 22.76 |
| 300 | 19.50 | 22.77 | 19.50 |
| 400 | 18.04 | 20.20 | 17.82 |
| Mean fertilizers | 21.63 | 24.12 | 21.63 |

**Tabela S5**. Regression models for dry matter and maize and soybean contents. Map; MAPHA (1 %); MAPZnBC (1 %).

| Fertilizers | Regression equations | $R^2$ |
|---|---|---|
| | Maize dry matter production aerial part (g $pot^{-1}$) | |
| Map | $y=14.5+0.08^{***}x-0.0001^{**}x^2$ | 0.99 |
| MAPZnBC | $y=15.5+0.1^{***}x-0.0002^{**}x^2$ | 0.92 |
| MAPHA | $y=15.2+0.06^{***}x-0.0001^{**}x^2$ | 0.86 |
| | Shoots maize P uptake (mg $vase^{-1}$) | |
| Map | $y=18.1+037^{***}x$ | 0.98 |
| MAPZnBC | $y=25.0+0.35^{***}x$ | 0.95 |
| MAPHA | $y=20.1+0.43^{***}x$ | 0.97 |
| | Soybean shoots dry matter (g $pot^{-1}$) | |
| Map | $y=12.31+0.03^{***}x$ | 0.75 |
| MAPZnBC | $y=10.94+0.24^{***}x$ | 0.89 |
| MAPHA | $y=11.37+0.03^{***}x$ | 0.92 |
| | Soybean shoots P uptake (mg $vase^{-1}$) | |
| Map | $y=15.64+0.15^{***}x$ | 0.88 |
| MAPZnBC | $y=9.52+0.17^{***}x$ | 0.98 |
| MAPHA | $y=13.90+0.17^{***}x$ | 0.95 |
| | Total shoots dry matter (g $pot^{-1}$) | |
| Map | $y=25.37+0.14^{***}x-0.0002^{***}x^2$ | 0.94 |
| MAPZnBC | $y=25.16+0.14^{***}x-0.0002^{***}x^2$ | 0.96 |
| MAPHA | $y=25.06+0.14^{***}x-0.0002^{***}x^2$ | 0.95 |
| | Total P uptake (mg) | |
| Map | $y=33.75+0.52^{***}x$ | 0.97 |
| MAPZnBC | $y=34.51+0.52^{***}x$ | 0.97 |
| MAPHA | $y=33.97+0.60^{***}x$ | 0.97 |

The significance of the regression coefficients was evaluated by the t test, after correcting the QMR of the general anova using the Fcalc software.

# GENERAL CONCLUSION

The chemical impregnation with $ZnCl_2$ showed to be a promising path to chemical activation for eucalypt biomass. The ZnBC produced under the study conditions presented high values of surface area and P adsorption capacity.

The coating of MAP granules with organic materials such as HA and ZnBC in different proportions did not show effectiveness to change the MAP diffusivity in the two studied soils, being observed that these materials do not have physical properties to coat the granules in order to change the diffusivity.

When the MAPHA and MAPZnBC treatments were evaluated in the granulesphere region, they showed potential to increase P recovered by soil, demonstrating that ZnBC is able to alter part of the P availability solubilized by MAP. Also, HA can act in the region surrounding the granule on the soil surface, decreasing the P adsorption. The treatments evaluated in a greenhouse experiment, only the MAPHA showed a positive significant difference for the total P content in the two crop cycles. Both materials present characteristics of interest for the management of P in weathered soils, demonstrating the potential to act as P sorption conditioners in these soils.